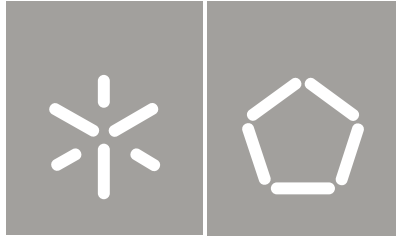Universidade do Minho
Escola de Engenharia

Cândida Sofia Teixeira Ferreira

Preparation and characterization of biodegradable blends of Poly(L-lactic) acid and Chitosan

Novembro de 2012

Universidade do Minho
Escola de Engenharia

Cândida Sofia Teixeira Ferreira

Preparation and characterization of
biodegradable blends of Poly(L-lactic)
acid and Chitosan

Novembro de 2012

# Acknowledgements

Firstly, I would like to thank Professor Natália Alves, my supervisor for giving me the opportunity of work at 3B's research group and improve my knowledge in biomaterials world. I must also thank her for all the support in this project. I am so very grateful for the help with every aspect of this research, from teaching about research methods, to scientific writing, and data analysis.

A very special appreciation to Sofia Caridade for all the help with the DMA technique.

I also want to thank to my dear colleague and friend Ana Cibrão for the help in the lab and outside of it. Thank you to my colleagues and friends of Materials Engineering.

I would like to make a special thanks to Cristina, Nuninho, Francisco and Tiago, my dear friends who were of foremost importance during this time of my life.

 The last but not the least, I want to thank very much my parents for all the help and comprehension during this work, without them this couldn't have been done. Also a big thank you to my boyfriend Diogo for being so comprehensive and supportive in this time of my life

**Acknowledgements**

## Abstract

Poly-(L-lactic acid) (PLLA) has been widely used for various biomedical applications due to its properties such as its biocompatibility, biodegradability, processability and its mechanical behaviour. Blending this polymer with chitosan (CHT) that, besides being biodegradable and hydrophilic, can interact with anionic glycosaminoglycans, proteoglycans and other negatively charged molecules of the extracellular matrix, could represent a good way to improve the biological performance of PLLA in these kinds of applications. When the PLLA_CHT blends are combined with success we hope that the CHT improves the biological properties of PLLA, and in the other hand, that the PLLA improves the mechanical properties of CHT.

The present work reports the optimization of a method for the preparation of PLLA and CHT blends, previously developed at 3B's research group. This method uses a common solvent for the two polymers, hexafluor-2-propanol (HFIP), to produce a homogeneous solution containing PLLA and CHT and the obtention of the films by solvent casting. Films with different fractions of each component were successfully prepared with the optimized method and didn't show visible phase separation. The effect of the blend composition on the wetability and morphology of the films was investigated by contact angle (CA) measurements and scanning electron microscopy (SEM), respectively. Swelling measurements were also conducted on the prepared samples. The influence of the blend composition on their thermal properties and miscibility was analysed by differential scanning calorimetry (DSC). Isothermal crystallization studies were also performed by DSC in order to enhance the comprehension about the effect of the presence of the CHT fraction on the PLLA crystallization process. The miscibility of the films as a function of their composition was evaluated in further detail by optical microscopy (OM) and Fourier transform infrared (FTIR) spectroscopy imaging.

Moreover, the viscoelastic behaviour of the developed PLLA_CHT films was studied for the first time by dynamical mechanical (DMA) in an unconventional way. Namely the mechanical properties of these films were measured while they were immersed in gradient compositions of water/ethanol mixtures. This procedure allowed the analysis of the glass transition dynamics of the CHT fraction, which would not be possible with conventional DMA tests. DMA temperature scans for the samples in the wet state were also conducted.

The prepared films evidenced a good miscibility at a microscope level. Moreover, it was found that crystallization is almost suppressed when the CHT fraction is equal or above 50%. Regarding the DMA results, it was possible to observe that the PLLA presence in the films improved their storage modulus.

# Resumo

O Poli(ácido láctico) (PLLA) tem sido bastante usado em várias aplicações biomédicas devido ás suas propriedades como a sua biocompatibilidade, biodegrabilidade e as suas propriedades mecânicas. Combinando este polímero com o quitosano (CHT) que além de ser biodegradável e hidrofilico, interatua com moléculas da matriz extracelular carregadas negativamente, pode ser uma boa maneira de melhorar a performance biológica do PLLA neste tipo de aplicações. Quando combinadas com sucesso, as membranas de PLLA_CHT espera-se que o CHT melhore as propriedades biológicas do PLLA, e que, o PLLA melhore as propriedades mecânicas do CHT.

Este trabalho apresenta a optimização de um método de preparação de misturas contendo PLLA e CHT desenvolvido no grupo de investigação 3B's. Este método simples de preparação dos filmes de PLLA e CHT utiliza um solvente comum aos dois polímeros, o hexafluor-2-propanol (HFIP) para produzir uma solução homogénea contendo PLLA e CHT. Os filmes foram obtidos por evaporação de solvente. Foram preparados com sucesso filmes com diferentes composições de cada componente da mistura que não apresentavam separação de fases a nível macroscópico. O efeito da composição dos filmes na sua molhabilidade e na sua morfologia foi analisada através da medição de ângulos de contacto (CA) e microscopia eletrónica de varrimento (SEM) respectivamente. A influência da composição dos filmes nas suas propriedades térmicas e na sua miscibilidade foi analisada por calorimetria diferencial de varrimento (DSC). Estudos da cristalização isotérmica foram efectuados por DSC com o intuito de perceber o efeito da fração de CHT na cristalização do PLLA. A miscibilidade dos filmes foi analisada com mais detalhe por microscopia óptica (OM) e análise de imagem da espectroscopia de infravermelho por transformada de Fourier (FTIR).

O comportamento viscoelástico dos filmes de PLLA_CHT foi analisado por análise mecânica dinâmica (DMA) através de um método não convencional. Neste método, as propriedades mecânicas dos filmes foram medidas com estes imersos em misturas de água/etanol. Esta análise possibilitou a perceção da dinâmica de transição vítrea da fração de CHT, o que não seria possível com os testes convencionais de DMA. Foram também realizados varrimentos de temperatura com as amostras molhadas.

Os filmes preparados evidenciavam uma boa miscibilidade a nível microscópico. Além disso, observou-se que o processo de cristalização é praticamente suprimido quando a fração de CHT nos filmes é igual ou superior a 50%. Em relação aos resultados de DMA, foi possível observar que a presença de PLLA nos filmes melhora o seu módulo de elasticidade

# Contents

## List of abbreviations

**C**

CHT – chitosan

**D**

DSC – Differential Scanning Calorimetry

DMA – Dynamical Mechanical Analysis

**E**

*E'* – Storage Modulus

**F**

FTIR - Fourier Transform infrared Spectroscopy

**H**

$\Delta H_c$ – Crystalization heat

$\Delta H_f$ – Melting heat

HFIP – Hexafluor-2-propanol

**O**

OM – Optical microscopy

**P**

PBS - phosphate buffered saline

PDLA – Poly (D-lactic acid)

PDLLA – Poly (DL-lactic acid)

PLA – Poly (lactic acid)

PLLA – Poly (L-lactic acid)

**S**

SEM – Scanning electron microscopy

**T**

Tan $\delta$ – Damping factor

Tc – Crystalization Temperature

Tg – Glass Transition Temperature

Tm – Melting Temperature

# List of figures

# List of Tables

# Chapter 1. General Introduction

## 1.1. Motivation and Content

Over the past two decades polymers from renewable resources have been attracting increasing attention on the modern medicine [1]. Investigations about materials for biomedical application are always looking for biomaterials and procedures for engineering materials properties adaptable to physiological requirements [2].

In this work, Poly(L-lactic) acid/Chitosan blends will be prepared by a simple methodology based on solvent casting, using a common solvent. The purpose of blending these two polymers is to combine the advantages of both synthetic (PLLA) and natural (CHT) polymeric classes. It is expected that these blends would present great potential for biomedical applications due to the combination of the properties of both PLLA and CHT.

The present chapter will present an overview of the research on biodegradable polymers and their use in biomedical applications.

## 1.2. Biodegradable Polymers

Nowadays, polymers have became a very important part of daily life. Biodegradable polymers have a special interest because they don't accumulate in nor harm the environment and thus can be considered "green" [3].

A polymer is biodegradable when it can be metabolized in biological environments, when living cells or microorganisms are present around the polymers. This metabolization process occurs in natural and microbiologically active environments like soils, seas, rivers, and lakes on the earth as well as in the body of human beings and animals [4]. In a strict sense, polymers that require enzymes of microorganisms for hydrolytic or oxidative degradation are regarded as biodegradable polymers [4,5]. Generally, a polymer that loses its weight over time in the living body is called an absorbable, resorbable, or bioabsorbable polymer as well as a biodegradable polymer, apart from both enzymatic and non-enzymatic hydrolysis [5].

The use of biodegradable polymers has increased in a vast range of applications but presently, biodegradable polymers have two main applications, one is the biomedical polymers that supply for medical care of the patients, and the other one is as ecological polymers that

keep the earth environments clean. As we can see in figure 1.1, most of the currently available biodegradable polymers are used for either of the two purposes, but some of these are applicable for both of them [3,5].
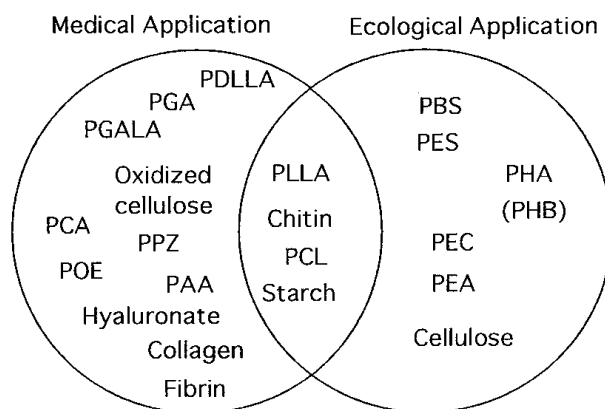


Figure 1.1. Application of biodegradable polymers. Adapted from [6].

Biodegradable polymers have been very used in biomedical applications. In fact, it has been developed a whole new generation of "polymer therapeutics" because of the large applicability of these polymers in tissue engineering and regenerative systems [6-10] In the design of these kind of materials some aspects should be taken into account [11], such as:

- They should not evoke a sustained inflammatory response;
- The degradation rate should be adequate for their function;
- They should have appropriate mechanical properties for their planned use;
- They should produce nontoxic degradation products that can be readily resorbed or excreted;
- They shoud have permeability and processability appropriate for designed application of the biomaterial

The above mentioned properties are affected by some factors such as molecular weight, surface charge, water adsorption, material chemistry, hydrophobicity, erosion mechanism and degradation.

These polymeric biomaterials are advantageous because they would naturally degrade and disappear in tissues over a desired period of time, this doesn't happen with nonbiodegradable devices that would permanently remain in biological tissues if not removed surgically [3].

Biodegradable polymers can be classified on the basis of the origin as synthetic or naturals. This classification is shown in table 1.1 [5].

Table 1.1. Classification of biodegradable polymers. Adapted from [5].

| Natural Polymers | | Synthetic Polymers | |
|---|---|---|---|
| Sub-classification | Examples | Sub-classification | Examples |
| 1.Plant origin<br>1.1 Polysaccharides | Cellulose, starch, Alginate | 1 Aliphatic polyesters<br>1.1 Glycol and dicarbonic acid polycondensates | Poly(ethylene succinate), Poly(butylenes terephthalate) |
| 2.Animal origin<br>2.1 Polysaccharides | Chitin (Chitosan), Hyalutonate | 1.2 Polylactides | Polyglycolide, Polylactides |
| 2.2 Proteins | Collagen (gelatin), Albumin | 1.3 Polylactones | Poly(e-carpolactone) |
| | | 1.4 Miscellaneous | Poly(butylene terephthalate) |
| 3 Microbe origin<br>3.1 Polyesters | Poly(3-hydroxyalkanoate) | 2 Polyols | Poly(vinyl alcohol) |
| | | 3 Polycarbonates | Poly(ester carbonate) |
| 3.2 Polysaccharides | Hyaluronate | 4 Miscellaneous | Polyanhydrides, Poly(a-cyanoacrylate)s, Polyphosphazenes, Poly(orthoesters) |

## 1.2.1. Natural Polymers

Natural polymers are produced in nature by all living organisms and are typically more chemically and structurally complicated than synthetic polymers [12,13].

Several natural polymers have been proposed for many applications in Tissue Engineering and Regenerative Medicine due to their properties. Some of the typical characteristics of these materials are the low citotoxicity, the easy biodegradation through normal metabolic pathways, and low immunogenic reaction upon implantation and the countless properties obtained by the combination with other biodegradable polymers [14].

Natural polymers complete a diverse set of functions in their native setting. For example, proteins function as structural materials and catalysts, polysaccharides function in membranes and intracellular communication, and lipids function as energy stores and so on [1].

Natural polymers can be grouped generally in three main classes: proteins, polysaccharides and bacterial polyesters. Table 1.2 shows some examples of natural polymers and their properties.

Table1.2. General Properties of Certain Natural Polymers. Adapted from [8].

|  | Polymer | Incidence | Physiological function |
|---|---|---|---|
| **A. Proteins** | Silk | Synthesized by arthropods | Protective cocoon |
|  | Keratin | Hair | Thermal insulation |
|  | Collagen | Connective tissues (tendon, skin, etc.) | Mechanical support |
|  | Gelatin | Partly amorphous collagen | (Industrial product) |
|  | Fibrinogen | Blood | Blood clotting |
|  | Elastin | Neck ligament | Mechanical support |
|  | Actin | Muscle | Contraction, motility |
|  | Myosin | Muscle | Contraction, motility |
| **B.Polysaccharides** | Cellulose (cotton) | Plants | Mechanical support |
|  | Amylase | Plants | Energy reservoir |
|  | Dextran | Synthesized by bacteria | Matrix for growth of organism |
|  | Chitin | Insects, crustaceans | Provides shape and form |
|  | Glycosaminoglycas | Connective tissues | Contributes to mechanical support |
| **C.Polynucleotides** | Deoxyribonucleic acids (DNA) | Cell nucleus | Direct protein biosynthesis |
|  | Ribonucleic acids (RNA) | Cell nucleus | Direct protein biosynthesis |

### 1.2.1.1. Proteins

Proteins are one of the essential macromolecules in biological systems and can be isolated easily from natural resources [1]. They are polyamides with α-amino acids as monomer units. Proteins are more complex than polyssacharides due to the large group of α-amino acids that exists naturally, which can form an almost limitless number of sequential arrangements [15]. Amino acids (Figure1.2) can be neutral like glycid, acidic as aspartic acid, or basic as lysine [1].
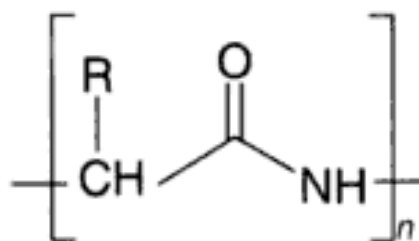


Figure 1.2. Amino acid structure. Adapted from [16]

Proteins have four levels of structure organization. The primary structure refers to the sequence of amino acids in the polypeptide chain; the secondary structure refers to the extended or helically coiled conformation of the polypeptide chains; the tertiary structure refers to the manner in which polypeptide chains are folded to form a tightly compact structure of globular protein, and the quaternary structure refers to how subunit polypeptides are spatially organized [1].

Proteins can be divided in fibrous and globular. Fibrous proteins are held together as fibrils by hydrogen bonds what makes them ideal to be applied as structural materials of animal tissues. Examples of fibrous proteins are collagens, elastins and fibroins. Globular proteins are ideal for functions that require mobility because they are dilute salts solutions or soluble in water through their peptide bonds or through their amino acid side-chains, and they are compact and folded. Examples of globular proteins are hormones or enzymes [1,15].

Collagen is the principal protein component of tendons, skin, blood vessels and bones [17]. Among the characteristics of collagen are good biocompatibility, high mechanical strength, low antigenicity and ability of crosslinking that enables the tailoring of the degradation, mechanical and water uptake properties [18].

Albumin is a protein found in plasma that has been used for many years in the treatment of burned patients and to restore the blood volume in patients with a low protein levels [15]. When attached on blood-contact biomaterials surfaces, albumin molecules can improve blood compatibilities. Due to its good blood compatibility, albumin has been evaluated as a carrier matrix [19].

Silk fibroin is a protein produced by spiders and some insects. Because of its reproducibility, nontoxicity, and environmental and biological compatibility, silk fibroin has been widely used in biomedical and biotechnological fields [16,20-22].

## 1.2.1.2. Polyssaccharides

Polyssacharides are constituted by sugar monomers and they can be obtained by different sources: animal sources such as chitosan, vegetal sources such as starch, and microbial sources such as dextran [23].

Polysaccharides are widely used in biomedical applications due to their biodegrability, biological functions like immune recognition. They have been blended with synthetic polymers to improve their mechanical properties [24].

Starch is composed by amylase and amylopectin, and the amylase/amylopectin ratio varies according to its age or origin. The amylase molecule is essentially linear and the amylopectin, on the other hand, is much branched [1,16]. The most available common starch existing is isolated from grains (rice, wheat, corn) and from tubers (potato and tapioca) [1]. Starch has been lended with other biomaterials to overcome problems like its difficulty to process, moisture sensitiveness, brittleness and poor mechanical properties [25-28]. Starch can be used in drug delivery systems and controlled release matrix systems [16].

Chitosan (CHT), is a natural polymer commonly obtained by alkaline hydrolysis of chitin, which after cellulose is the most abundant natural polymer [5]. Chitin can be found in shells of crustaceans like crabs and shrimp, cell walls of funghi and cuticles of insects [29. Chitosan derives from the deacetylation of chitin (Figure 1.3), and can be found in a wide range of molecular weight and degree of deacetylation [30]. CHT is non-toxic, biocompatible, hemostatic and biodegradable hydrophilic and polycationic. Due to its interesting characteristics, CHT has been proposed for biomedical and drug delivery applications [30-35].
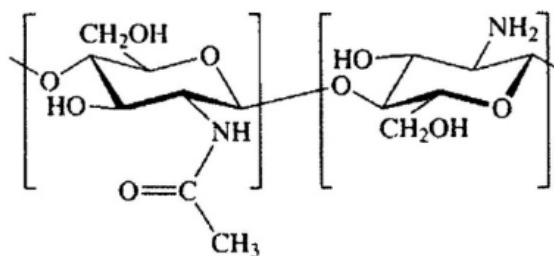
Figure 1.3. Structure of partially acetylated chitosan. Adapted from [36].

Dextran is a polysaccharide that belongs to the family of homopolysaccharides. Dextran is slowly degraded, highly biocompatible, innocuous to the body and readily excreted from it. Because of these characteristics, dextran has been used in biomedical applications [12,32]. Moreover, dextran and its derivatives have been used in nutrition applications, additives in bakery, candies and ice creams [12].

### 1.2.1.3.  Bacterial Polyesters

Bacterial polyesters are produced by a variety of microorganisms in response to nutrient limitation. When exposed to natural microorganisms in the ecosystem, biodegradable polyesters suffers degradation to water and carbon dioxide very fast, in about 1 to 6 months [17].

These polymers are interesting because of some of their properties like biocompatibility and biodegradability. Bacterial Polyesteres have been used in tissue engineering and being studied for Tissue Engineering (TE) applications in the form of nanofibers, films or 3-D scaffold [37-39].

## 1.2.2. Synthetic Polymers

Synthetic polymers began to be produced early in the twentieth century [1]. Presently, synthetic polymers have become an interesting alternative for biomedical applications due to a variety of properties that can be obtained with a proper design without altering the bulk properties [37]. They are generally inert and have personalized property profiles for specific applications [38]. Moreover, they can be designed purposely to remove the risk of immunogenicity and pathogenicity that can come with the use of some natural polymers [38].

Synthetic polymers can be divided in three broad groups: fibers such as nylon and terylens, synthetic rubbers like neoprene rubber, and plastics [39]. In the biomedical application field, the linear aliphatic polyesters and the polyhydroxyalkanoates are the most studied [40]. These two classes of polymers have been shown to be biocompatible and non-toxic [39]. Among aliphatic polyesters, two of the most used in biomedical applications are poly(lactic acid) and poly(glycolic acid).

In table 1.3 we can see examples of synthetic polymers.

Table 1.3. Examples of synthetic polymers. Adapted from [41].

| Type | Examples | Typical uses |
|---|---|---|
| **Plastics** | Polystyrene, poly(methyl methacrylate), poly(vinyl chloride) | Bottles, toys, seemingly everything |
| **Fibers** | Nylon, polyesters, polyamids | Clothing, disposable diapers, tennis raquets, carpets, fishing line |
| **Films** | Polyethylene, polyesters | Packaging, grocery and garbage bags, paints, photographics films |
| **Elastomers** | Polybutadiene, polyisoprene | Tires, golf balls, condoms, latex gloves, rubber bands |
| **adhesives** | Epoxies, poly(vinyl alcohol), polycyanoacrylates | White glue, epoxy cement, "instant" glue |

Poly(lactic acid) (PLA) is composed by lactic acid, which is produced by fermentation of carbohydrates. Lactic acid exists in two optical active forms: L-lactide and D-lactide. PLA is a high modulus and high strength polymer that can easily be processed by extrusion, injection, blow moulding, and thermoforming. Its degradation depends on distinct factors such as temperature, time or weight impurities [41]. PLLA is biodegradable and non-toxic to the human body and to the environment. Due to these properties, PLA has been studied for biomedical and

pharmaceutical applications [1]. In the biomedical applications PLLA of high molecular weight is preferred, and in the other hand, in pharmaceutical applications PLLA of low molecular weight is preferred [41]. Among biomedical applications of PLLA are drug delivery, artificial organs supports in tissue engineering [42,43]

Poly(glycolic acid) (PGA), figure1.4, is a rigid thermoplastic with a high cristallinity. This polymer is produced in a variety of forms and structures by various processes that affect its properties and degradation characteristics. Some of these processes are injection, extrusion, solvent casting and compression moulding. The mainly interesting characteristic of PGA as a material for biomedical applications is the fact that its degradation products are natural metabolites. The main application of PGA is in resorbable sutures [41].
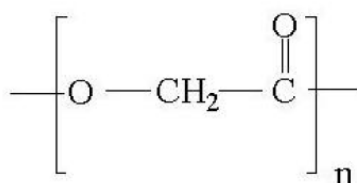


Figure 1.4. PGA monomer. Adapted from[44]

## 1.3.  Natural and Synthetic Polymer Blends

A polymer blend (Figure 1.5) is defined as any physical mixture of two or more polymers or copolymers that are not linked by covalent bonds [36].
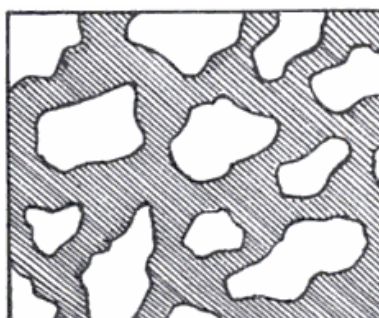


Figure 1.5. Scheme of a polymer blend, showing  dispersed phase of a polymer in the continuous phase of another one. Adapted from [40].

In the last few years, there has been an economic interest in blending polymers since the development of a new polymer to meet a specific need is quite expensive. Hence, if the desired

properties could be achieved simply by mixing two or more polymers, that would be an advantage [15].

There are various types of polymer blends: mechanical blends, mechanochemical blends, latex blends, solution-cast blends, and chemical blends as it is shown in Table 1.4.

Table 1.4.Types of polymer blends. Adapted from [15]

| Type of blend | Description |
|---|---|
| **Mechanical blends** | Polymers are mixed at temperatures above Tg or Tm for amorphous or semicrystalline polymers, respectively. |
| **Mechanochemical blends** | Polymers are mixed at shear rates high enough to cause degradation. Resultant free radicals combine to form complex mixtures including block and graft components. |
| **Solution-cast blends** | Polymers are dissolved in common solvent and solvent is removed. |
| **Latex blends** | Fine dispersion of polymers in water (latexes) are mixed, and the mixed polymers are coagulated |
| **Chemical blends** | |
| **Interpenetrating polymer networks (IPN)** | Crosslinked polymer is swollen with different monomer, then monomer is polymerized and crosslinked. |
| **Semi-interpenetrating polymer networks (semi-IPN)** | Polyfunctional monomer is mixed with thermoplastic polymer, then monomer is polymerized to network polymer. |
| **Simultaneous interpenetrating polymer networks (SIN)** | Different monomers are mixed, then homopolymerized and crosslinked simultaneously, but by noninteracting mechanisms. |
| **Interpenetrating elastomeric networks (IEN)** | Latex polyblend is crosslinked after coagulation. |

The biomedical field has a big interest in combining polymers to obtain better results. Hence, the properties of a natural polymer can be improved when blended with an adequate synthetic polymer. In biomedical applications, the disadvantage of many synthetic polymers, biocompatibility, is exactly the advantage of natural polymers. In these cases, natural polymers improve the biological properties of synthetic polymers [15].

## 1.3.1. PLLA/CHT Blends

Blending natural and synthetic polymer is a good way to improve the blended polymers properties, as mentioned before In this work PLLA and CHT were blended.

Recently, CHT and its derivatives have been widely used in different biomedical applications like drug delivery systems, wound healing accelerators and nerve regeneration agents. As said before, it is hydrophilic and polycationic, due to the presence of amino and hydroxyl groups on its backbone, bioadhesive and presents antimicrobial activity. However, CHT poor mechanical properties and its insolubility in common organic solvents have delayed CHT basic research and some of its applications [33,45,46]. On the other side PLLA has been widely used in tissue engineering and drug delivery systems due to its good mechanical properties and biodegradability [34,47]. But its hydrophobicity and the absence of active cell recognition sites decrease its capability of hosting cells, while the acidic products from its degradation can cause inflammation when implanted. These drawbacks can be overcome with some strategies to modify the poly-(L-lactic) acid surface modification and improve is cytocompatibility like grafting techniques, hydrolysis, electrostatic self-assembly, coating of natural polymers, plasma treatment, ozone oxidation and some combinations of these techniques [53]. In addition to these techniques, we can blend polylactides with others natural or synthetic polymers and depending on their miscibility and eventual interaction at a molecular level, obtain desirable properties [42,49].

When blending PLLA and CHT successfully, the CHT/PLLA blend should be bioadhesive and hydrophilic and the mechanical properties of CHT in the wet state (i.e, when implanted) will be improved by the presence of the PLLA component. Moreover, the CHT component will buffer the acidic degradation products of PLLA. Yet, is not easy to mix chitosan with PLLA in a high miscible level due to two factors: the first is that CHT has a high $T_g$ and probably, it will decompose before melting and for this reason, is practically impossible to melt CHT and PLLA by melting-based processing techniques; the second reason is that are unknown common solvents for CHT and PLLA [50]. Nevertheless, some combinations of CHT and polylactides have been previously reported. Chen et al. have investigated PLLA/CHT blends [51]. These blends were obtained using dimethyl sulfoxide (DMSO) and acetic acid as solvents for PLLA and CHT, respectively, and directly precipitating in acetone. The thermal properties of the blends were studied, but $T_g$ and $T_m$ of CHT were not detected [51]. Suyatma et al. reported PLLA/CHT films [52], using 1% aqueous acetic acid solution as solvent for the CHT and chloroform for PLLA. The films have

been prepared via a solvent-casting method and dried in the air. However, there was no miscibility between the two components of the films because chloroform has poor solubility in water and also evaporates much more quickly than water from the casting membranes during the dry procedure [52]. Wan et al. have prepared some PDLLA/chitosan and PLLA/chitosan blend membranes using a two-step method. In the first step, solutions of each component were mixed and casted into a gelatinous membrane, and in the second step, the obtained membranes were introduced into a mixed solution for the solvent extraction followed by a drying process to generate the membrane. An acetic acid-acetone system was selected for the PDLLA/CHT membranes, and for the PLLA/CHT membranes was used a system of acetic acid and dimethyl sulfoxide. However, the prepared membranes still presented a phase separation at the microscopic level [50].

## 1.4. References

1. Yu, L., *Biodegradable Polymer Blends and Composites from Renewable Resources*. 2009: Wiley.

2. Kolhe, P. and R.M. Kannan, *Improvement in Ductility of Chitosan through Blending and Copolymerization with PEG: FTIR Investigation of Molecular Interactions*. Biomacromolecules, 2002. 4(1): p. 173-180.

3. Domb, A.J. and N. Kumar, *Biodegradable Polymers in Clinical Use and Clinical Development*. 2011: Wiley.

4. Rieger, B., A. Künkel, and G.W. Coates, *Synthetic Biodegradable Polymers*. 2012: Springer.

5. Ikada, Y. and H. Tsuji, *Biodegradable polyesters for medical and ecological applications*. Macromolecular Rapid Communications, 2000. 21(3): p. 117-132

6. Silva, G.A., P. Ducheyne, and R.L. Reis, *Materials in particulate form for tissue engineering. 1. Basic concepts*. Journal of Tissue Engineering and Regenerative Medicine, 2007. 1(1): p. 4-24.

7. Peniche, C., et al., *Chitosan: An Attractive Biocompatible Polymer for Microencapsulation*. Macromolecular Bioscience, 2003. 3(10): p. 511-520.

8. Ratner, B.D., A.S. Hoffman, and F.J. Schoen, *Biomaterials Science: An Introduction to Materials in Medicine*. 2004: Elsevier Science.

9. Khorasani, M.T., M. Zaghiyan, and H. Mirzadeh, *Ultra high molecular weight polyethylene and polydimethylsiloxane blend as acetabular cup material*. Colloids and Surfaces B: Biointerfaces, 2005. 41(2–3): p. 169-174.

10. Buford, A. and T. Goswami, *Review of wear mechanisms in hip implants: Paper I – General*. Materials &amp; Design, 2004. 25(5): p. 385-393.

11. Ulery, B.D., L.S. Nair, and C.T. Laurencin, *Biomedical applications of biodegradable polymers*. Journal of Polymer Science Part B: Polymer Physics, 2011. 49(12): p. 832-864.

12. Bastioli, C. and R.T. Limited, *Handbook of Biodegradable Polymers*. 2005: Rapra Technology.

13. Enderle, J. and J. Bronzino, *Introduction to Biomedical Engineering*. 2011: Elsevier Science.

14. Neves, N.M., *Biological performance of natural-based polymers for tissue engineering scaffolding.* Tissue Engineering Part A, 2008. 14(5): p. 705-705.

15. Stevens, M.P., *Polymer Chemistry: An Introduction.* 1998: Oxford University Press, USA

16. Vepari, C. and D.L. Kaplan, *Silk as a biomaterial.* Progress in Polymer Science, 2007. 32(8–9): p. 991-1007.

17. Barbucci, R., *Integrated Biomaterials Science.* 2002: Springer.

18. Mano, J.F., et al., *Natural origin biodegradable systems in tissue engineering and regenerative medicine: present status and some moving trends.* Journal of the Royal Society Interface, 2007. 4(17): p. 999-1030.

19. Theodore Peters, J., *All About Albumin: Biochemistry, Genetics, and Medical Applications.* 1995: Elsevier Science.

20. Unger, R.E., et al., *Growth of human cells on a non-woven silk fibroin net: a potential for use in tissue engineering.* Biomaterials, 2004. 25(6): p. 1069-1075.

21. Motta, A., et al., *Fibroin hydrogels for biomedical applications: preparation, characterization and in vitro cell culture studies.* Journal of Biomaterials Science, Polymer Edition, 2004. 15(7): p. 851-864.

22. Minoura, N., M. Tsukada, and M. Nagura, *Fine structure and oxygen permeability of silk fibroin membrane treated with methanol.* Polymer, 1990. 31(2): p. 265-269.

23. Cascone, M.G., et al., *Bioartificial polymeric materials based on polysaccharides.* Journal of Biomaterials Science, Polymer Edition, 2001. 12(3): p. 267-281.

24. Cascone, M.G., et al., *Dextran/poly(acrylic acid) mixtures as miscible blends.* Journal of Applied Polymer Science, 1997. 66(11): p. 2089-2094.

25. Ghosh, S., et al., *Bi-layered constructs based on poly(L-lactic acid) and starch for tissue engineering of osteochondral defects.* Materials Science & Engineering C-Biomimetic and Supramolecular Systems, 2008. 28(1): p. 80-86.

26. Santos, M.I., et al., *Response of micro- and macrovascular endothelial cells to starch-based fiber meshes for bone tissue engineering.* Biomaterials, 2007. 28(2): p. 240-248.

27. Gomes, M.E., et al., *Alternative tissue engineering scaffolds based on starch: processing methodologies, morphology, degradation and mechanical properties.*

Materials Science & Engineering C-Biomimetic and Supramolecular Systems, 2002. 20(1-2): p. 19-26.

28. Lam, C.X.F., et al., *Scaffold development using 3D printing with a starch-based polymer.* Materials Science and Engineering: C, 2002. 20(1–2): p. 49-56.

29. Lehermeier, H.J., J.R. Dorgan, and J.D. Way, *Gas permeation properties of poly(lactic acid).* Journal of Membrane Science, 2001. 190(2): p. 243-251.

30. Ravi Kumar, M.N.V., *A review of chitin and chitosan applications.* Reactive and Functional Polymers, 2000. 46(1): p. 1-27.

31. Menczel, J.D. and R.B. Prime, *Thermal Analysis of Polymers, Fundamentals and Applications.* 2009: Wiley.

32. Squire, J.R., *Dextran: its properties and use in medicine.* 1955: Blackwell Scientific Pub.

33. Liu, L., et al., *Preparation of chitosan-g-polycaprolactone copolymers through ring-opening polymerization of ϵ-caprolactone onto phthaloyl-protected chitosan.* Biopolymers, 2005. 78(4): p. 163-170.

34. Cai, Q., et al., *Synthesis and Properties of Star-Shaped Polylactide Attached to Poly(Amidoamine) Dendrimer.* Biomacromolecules, 2003. 4(3): p. 828-834.

35. Teegarden, D.M., Polymer Chemistry: Introduction to an Indispensable Science. 2004: NSTA Press, National Science Teachers Association

36. Dutta, P.K., J. Dutta, and V.S. Tripathi, *Chitin and chitosan: Chemistry, properties and applications.* Journal of Scientific & Industrial Research, 2004. 63(1): p. 20-31

37. Nair, L.S. and C.T. Laurencin, *Biodegradable polymers as biomaterials.* Progress in Polymer Science, 2007. 32(8-9): p. 762-798.

38. Meyer, U., et al., *Fundamentals of Tissue Engineering and Regenerative Medicine.* 2009: Springer.

39. Misra, G.S., *Introductory Polymer Chemistry.* 1993: J. Wiley & Sons.

40. Amass, W., A. Amass, and B. Tighe, *A review of biodegradable polymers: Uses, current developments in the synthesis and characterization of biodegradable polyesters, blends of biodegradable polymers and recent advances in biodegradation studies.* Polymer International, 1998. 47(2): p. 89-144.

41. Gupta, A.P. and V. Kumar, *New emerging trends in synthetic biodegradable polymers - Polylactide: A critique.* European Polymer Journal, 2007. 43(10): p. 4053-4074.

42. Wan, Y., et al., *Porous polylactide/chitosan scaffolds for tissue engineering.* Journal of Biomedical Materials Research Part A, 2007. 80A(4): p. 776-789.

43. Dechy-Cabaret, O., B. Martin-Vaca, and D. Bourissou, *Controlled Ring-Opening Polymerization of Lactide and Glycolide.* Chemical Reviews, 2004. 104(12): p. 6147-6176.

44. Hubbell, J.A., *Synthetic biodegradable polymers for tissue engineering and drug delivery.* Current Opinion in Solid State & Materials Science, 1998. 3(3): p. 246-251.

45. Wu, Y., et al., *Synthesis and characterization of a novel amphiphilic chitosan–polylactide graft copolymer.* Carbohydrate Polymers, 2005. 59(2): p. 165-171.

46. .Fujioka, M., et al., *Enzymatic Synthesis of Chitin- and Chitosan-graft-Aliphatic Polyesters.* Macromolecular Rapid Communications, 2004. 25(20): p. 1776-1780.

47. Tian, H.Y., et al., Biodegradable synthetic polymers: Preparation, functionalization and biomedical application. Progress in Polymer Science, 2012. 37(2): p. 237-280

48. Lin, Y., et al., *Surface modification of poly(l-lactic acid) to improve its cytocompatibility via assembly of polyelectrolytes and gelatin.* Acta Biomaterialia, 2006. 2(2): p. 155-164.

49. Alves, N.M., et al., *Preparation and Characterization of New Biodegradable Films Made from Poly(L-Lactic Acid) and Chitosan Blends Using a Common Solvent.* Journal of Macromolecular Science, Part B, 2011. 50(6): p. 1121-1129.

50. Wan, Y., et al., *Biodegradable Polylactide/Chitosan Blend Membranes.* Biomacromolecules, 2006. 7(4): p. 1362-1372

51. Chen, C., L. Dong, and M.K. Cheung, *Preparation and characterization of biodegradable poly(L-lactide)/chitosan blends.* European Polymer Journal, 2005. 41(5): p. 958-966.

52. Suyatma, N.E., et al., *Mechanical and barrier properties of biodegradable films made from chitosan and poly (lactic acid) blends.* Journal of Polymers and the Environment, 2004. 12(1): p. 1-6.

# Chapter 2. Materials and Methods

## 2.1. Materials

### 2.1.1. Chitosan

Chitosan (CHT) is a derivative of chitin, which is the most abundant natural amino polysaccharide and is expected to be produced almost as much as cellulose [1]. Chitin can be found mainly in the shells of crustaceans such as crab and shrimp, cell walls of funghi ans cuticles of insects [2].

Chitosan is the universal non-toxic N-de-acetylated derivative of chitin, where chitin is N-deacetylated to such an amount that it becomes soluble in aqueous acetic and formic acids. Chitosan is the fully or partially derivative of chitin with a usual degree of acetylation between 30 to 95% [1-4]. Chitosan solubility depends on the degree of deacetylation and pH. When chitosan has a degree of deacetylation of approximately 40%, it can be soluble in solutions with a pH of 9; however, when the degree of deacetylation is around 85% it can be soluble in solutions with pH of 6.5. The viscosity of a chitosan solution also depends on the degree of deacetylation. With the increase of viscosity there will be an increase of the degree of deacetylation. [5].

Chitosan is semicrystalline and its degree of crystallinity is dependent of the degree of deacetylation, being maximum when the degree of deacetylation is 100% [6]. It is commercially available in a large range of molecular weights and degrees of deacetylation[3].
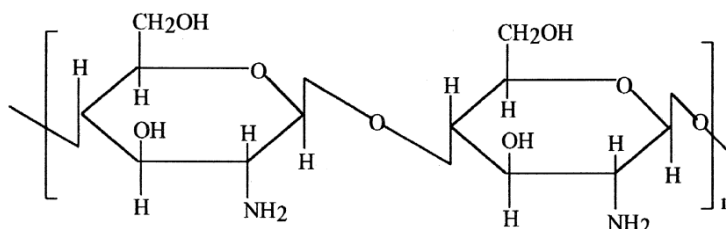


Figure 2.1. Chitosan structure. Adapted from [1].

The glass transition process in chitosan has been addressed in different works, but the results are far from being in agreement. Glass transition of chitosan, as in most of glass forming

materials, has been only studied in the temperature axis, or combinations of temperature and frequency. In this context, some thermal analysis technique have been employed to characterize the $T_g$ of chitosan, namely DMA and DSC [7-10]

Chitosan is non-toxic, non-antigenic, biodegradable and biocompatible [11]. It has been reported to have reactive functional groups and polyelectrolyte properties. It is also hemostatic, bioadhesive and has high adsorption capacity, anti-tumor influence, anti-microbial and anti-oxidative activity, analgesic effect and cell affinity [4,12,13].

Due to the above mentioned properties, chitosan and its derivates are being used in a huge variety of widely different products and applications range from cosmetics, food processing, biomedical applications [4]. Biomedical applications of chitosan includes wound healing and wound dressing, tissue engineering, burn treatment, artificial skin, ophthalmology and drug delivery systems [1].

In the work medium molecular weight chitosan was purchased from Aldrich and purified at the 3B's laboratory. The degree of deacetylation of the used chitosan was 80%.

## 2.1.2. Poly (L-lactic) acid

Poly–(L-lactic) acid (PLLA) is one of the stereoisomeric forms of polylactides [14]. The lactide monomer from polylactides comes from lactic acid, a fermentation product available from dextrose, which is obtainable from corn milling [15]. Polylactides belong to a family of aliphatic polyester and has two optically active forms of isomers, L- and D-lactic acid. After condensation, the isomers consisted of L-lactide, D-lactide and meso-lactid undergoing polymerization to produce poly-(L-lactic) acid (PLLA), poly-(D-lactic) acid (PDLA) or poly-(DL-lactic) acid (PDLLA) (Figure 2.2). The most common commercially polylactides are poly-(L-lactide) and poly-(D-lactide) [14]. Poly-(L-lactic) acid and poly-(DL-lactic) acid can be simply biodegradable into monomeric units of lactic acid by undergoing scission as a result of hydrolysis [13].
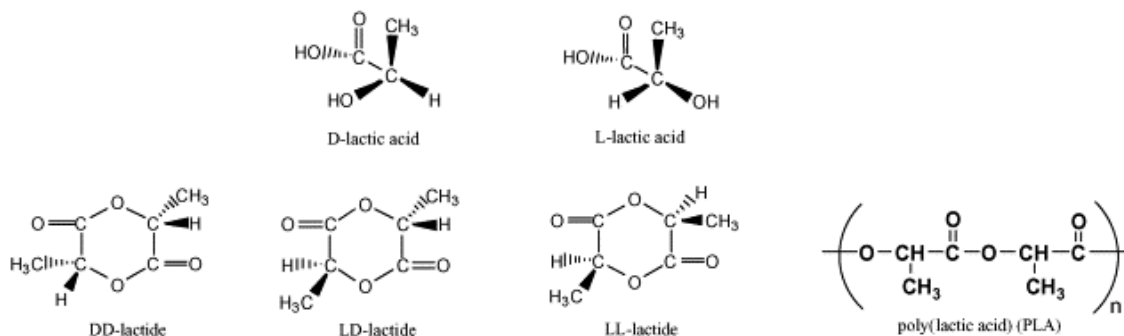
Figure 2.2. Chemical structure of Polylactide and its constituents. Adapted from [11].

Poly-(L-lactic) acid is typically semicrystalline. Its glass transition temperature (Tg), crystallinity, and melting temperature can change in a certain range that depends on the crystallization conditions, polymerization routes and the molecular weight of the resultant products [16].

Due to some of its properties such as its biocompability, its biodegradability, its absorbable characteristics and its good mechanical properties, poly-(L-lactic) acid as been widely used in environmental and biomedical applications [13,17,18].

Some of poly-(L-lactic) acid biomedical applications are related with artificial organs, drug delivery systems, ocular inserts, carriers of immobilized enzymes and cells, temporary implants for fixations and supports in tissue engineering [13,18].

In spite of the success of poly-(lactic) acid use, its application can be limited for some factors as well [14]:

- Relative brittleness at room temperature;
- acid degradation products , that causes a decline of local and systemic pH and results in some side effects like inflammatory response;
- hydrophobicity, hindering the cells from penetration into the scaffolds pores;
- absence of cell recognition sites on the surface of the scaffolds, leading to poor cell affinity and adhesion.

These drawbacks can be overcome with some strategies to modify the poly-(L-lactic) acid surface modification and improve is cytocompatibility like grafting techniques, hydrolysis, electrostatic self-assembly, coating of natural polymers, plasma treatment, ozone oxidation and

some combinations of these techniques [19]. In addition to these techniques, we can blend polylactides with others natural or synthetic polymers and depending on their miscibility and eventual interaction at a molecular level, obtain desirable properties [13,17].

Poly-(L-lactic) acid of low molecular weight was purchased from Purac.

## 2.2 Methods – Characterization Techniques

### 2.2.1. Differential Scanning Calorimetry

Differential scanning calorimetry (DSC) is the most widely used of available the thermal techniques, providing a fast and easy method of obtaining a wealth of information about a material, whatever the end use envisaged [20]. DSC is a calorimetry pure technique which measures directly the absorption of the heat energy that takes place in a sample during controlled increase or decrease of temperature [20-22].

The DSC is used in polymer research for mainly three different types of experiments [23]:

- ➢ glass transition temperature ($T_g$) measurements;
- ➢ melting and recrystallization temperature ($T_m$ and $T_c$) and heat determinations ($H_m$ and $H_c$);
- ➢ measurements on reacting systems

Figure 2.3 represens a typical DSC thermogram that shows the glass transition temperature ($T_g$), the crystallization temperature ($T_c$) and the melting temperature ($T_m$):
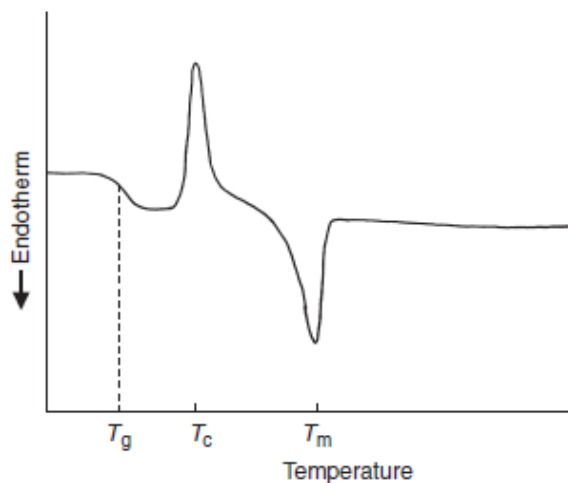
Figure 2.3. DSC thermogram showing the glass transition temperature (Tg), the crystallization temperature (Tc), and the melting temperature (Tm). Adapted from[24].

DSC (Figure 2.4) is commercially available in two basic types (Figure 2.4), the power-compensation DSC and the heat flow DSC. Both types of DSC have a common characteristic, the measure signal is proportional to a flow rate and not to a heat. This allows time dependences of a transition to be observed on the basis of the flow rate curve. This fact enables all DSCs to solve problems arising in many fields of applications [25].

In the heat flux DSC is used one single heater to increase the temperature of the sample and the reference cell. The small temperature differences taking place due to exothermic or endothermic effects in the sample are recorded as a function of the programmed temperature [23].

In the power-compensation energy DSC (figure 2.4) experiments there are two practically identical cells, one for the sample and the other one for the reference. Both, sample and reference are heated with separated heaters whose temperatures are measured with different sensors[20,22].

**(a)**
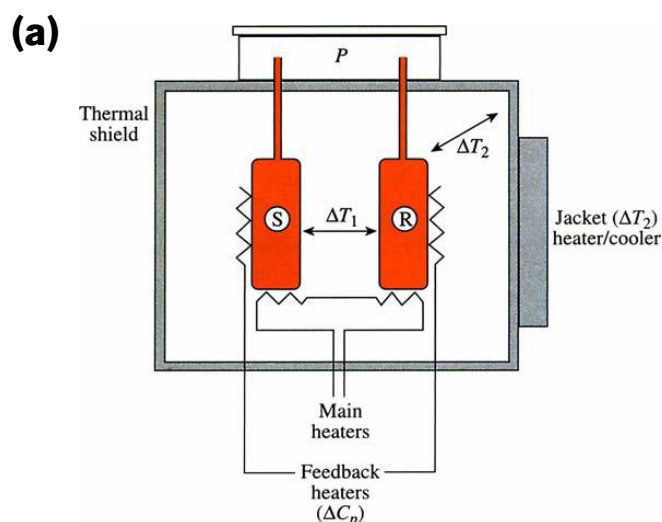


Figure 2.4 a. Layout of a typical heat flux DSC. Adapted from [21].

**(b)**
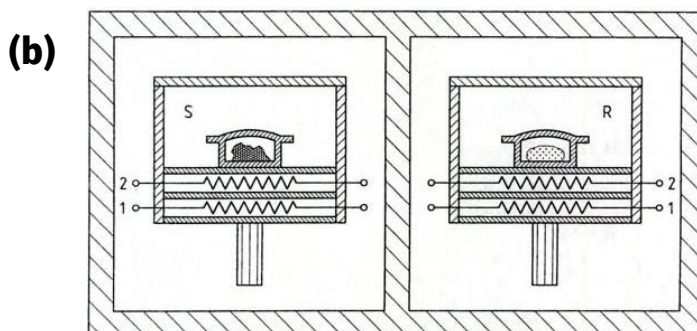


Figure 2.5 b. Power compensated DSC, where 1 is the heating wire and 2 is the resistence thermometer. Adapted from [25].

## 2.2.2. Dynamical Mechanical Analysis

Dynamical Mechanical Analysis (DMA) is a technique in which the elastic and viscous response of a sample under an oscillating load are monitored under time, frequency or temperature. The DMA technique is used to investigate the amorphous phase of polymers and offers an excellent sensitivity to measure the phase transition effects and is especially useful for the investigation of secondary relaxation effects and for the determination of "weak" glass-ruber transition effects [23].

The DMA technique can be simply described as the application of an oscilattory strain force to a sample and analysis of the material's stress response to that force. After the material response measure, the phase angle δ, or phase shift between the force application and response is measured [26,27]. This principle is illustrated in figure 2.5. The samples are subjected to a cyclic deformation at a fixed frequency ranging from 1 to 1000Hz. The stress (σ) response is measured while the cyclic strain (ε) is applied and the temperature is increasing slowly. If the strain is a sinusoidal function of time given by:

$$\varepsilon(\omega) = \varepsilon_0 * \sin(\omega t) \qquad\qquad (1)$$

Where **ε** is the time-dependent strain, $\varepsilon_0$ the strain amplitude, ω the frequency of oscillation, and t the time, the result stress can be expressed by:

$$\sigma(\omega) = \sigma_0 * \sin(\omega t + \delta) \qquad\qquad (2)$$

Where **σ** is the time-dependent stress, $\sigma_0$ the amplitude of the stress response, and δ the phase angle between stress and strain. For Hookean solids, the stress and strain are completely in phase (δ=0), while for pure viscous liquids, the stress response lags by 90°. Real materials demonstrate viscoelastic behavior where δ has a value between 0° and 90°.
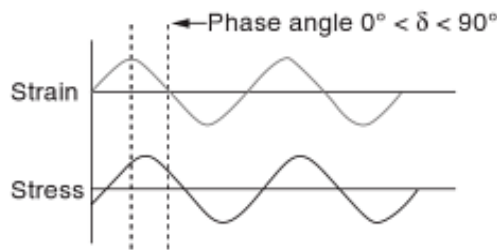


Figure 2.6. Basic principle of DMA. Application of an oscillatory strain to the sample and resulting sinusoidal stress measurement. Adapted from [26].

In DMA, a complex modulus (E*), an elastic modulus (E') and an imaginary loss modulus (E'') are calculated from the material response to the sine wave. These modulus allows a better characterization of the material because we can now analyse the ability of the return energy (E') and to lose energy (E''), and with this two values we can calculate the damping factor:

$$E^* = E' + iE''$$  (3)

$$\tan \delta = \frac{E''}{E'}$$  (4

The DMA is used to detect transitions resulting from molecular motions or relaxations, to determine mechanical properties such as the storage modulus (E') and the damping factor (tan δ) and to understand structure-property or morphology relationships [26].

## 2.2.3. Contact Angles Measurements

A wetting system is characterized by the contact angle that can be defined as the quantitative measure of the wetting of a solid by a liquid and is believed to be the straightforward and simplest method to obtain surface properties. A low contact angle means that the solid is well wetted by the liquid (hydrophilic solid surface), while a high contact angle means a preference for solid-fluid contact (hydrophobic solid surface) [28-30]. Of the vast array of methods for measuring the contact angles, the most common is to observe a sessile drop with a telescope microscope [31].

When considering a liquid drop that is placed on a solid surface as shown in figure 2.6, the drop is in equilibrium by balancing three forces:, the interfacial tensions between solid and liquid ($\gamma$SL), solid and vapor ($\gamma$SV) and between liquid and vapor ($\gamma$LV). The contact angle (θ) is the angle formed by a liquid drop at the three-phase boundary where the liquid, gas and solid intersect and it is included between the tangent plane to the surface of the liquid and the tangent plane to the surface of the solid at the point of intersection [29].
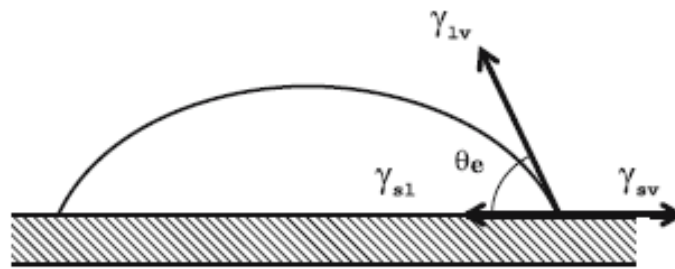
Figure 2.7. Vectorial equilibrium for a drop of a liquid on a solid surface. Adapted from [24].

The contact angle equilibrium was discovered by Young in 1805 and the vectorial sumatory of the forces at the three-phase boundary intersection point can be described by fowling equation,

$$\gamma SV = \gamma SL + \gamma LV \cos \theta \tag{5}$$

Where, $\gamma$ is the surface free energy term [31]. The energy of the surface is directly related to wettability and his is a useful parameter frequently associated with biological interaction. Even though $\gamma SV$ cannot be directly obtained since the equation above contains two forces unknown, $\gamma SL$ and $\gamma SV$. For that reason, $\gamma SV$ is usually approximated by the Zisman method for obtaining the critical surface tension. The Zisman method allows an approximation to the solid surface tension to be measured [30]..

From the point of view of the thermodynamic equilibrium, partial and complete wetting are two different things, figure 2.7.
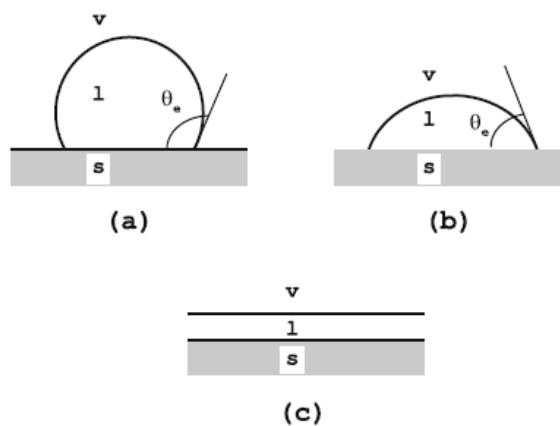


Figure 2.8. Different wetting situations of a liquid drop in contact with a solid surface. (a) and (b) correspond to partial wetting and (c) to a complete wetting. Adapted from [28]

Complete wetting means that the contact angle between a liquid and a solid interface is zero, $\theta=0$ [24]. Partial wetting occurs when the contact angle is finite, $\theta>0$. When $\theta$ is lower than 90° the liquid partially wets the solid and if is higher than 90° the liquid is said to be non-wetting [28,29].

The form of the liquid drop is determined by a combination of surface tension and gravity effects. A surface force tends to make spherical drops, whereas gravity tends to flatten a sessile drop or to elongate a pendant drop [28].

## 2.2.4. Optical Microscopy

Optical microscopy is one of the primary tools for the morphological characterization of microestruture in science, medicine and engineering [32]. With help of digital video, optical microscopy can be used to image very thin optical sections [33,34].

The optical microscope, figure 2.8, an optical instrument that uses visible light to produce a magnified image of an object that is projected on top of the retina of the eye or onto an image device. The two lenses, the objective and the ocular lens work together to produce the final magnification M of the image such that [2]:

$$M_{final} = M_{obj} \times M_{.oc} \tag{6}$$
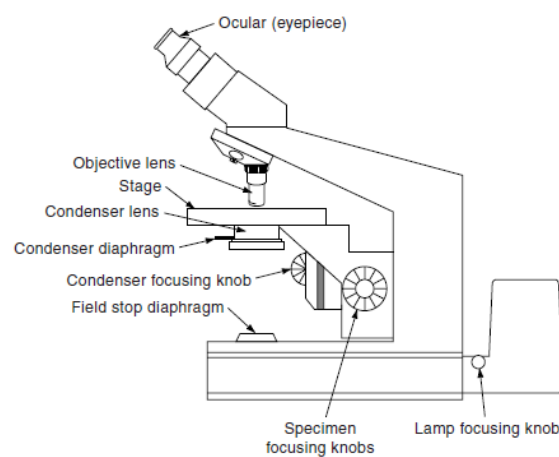


Figure 2.9. The compound light microscope. Adapted from [35].

In case of forming image, two microscope components are of critical importance, the objective lenses and the condenser lenses. The first one collects the light diffracted by the specimen and forms a magnified real image at the real intermediate image plane near the eyepieces or oculars, and the second focuses light from the illuminator on top of a small area of the specimen. Both components contain multiple lens elements that perform close to their hypothetical limits and are therefore expensive [35].

The lens of an optical magnifying glass forms an image of an object due to the refractive index of glass that is much bigger than that of the atmosphere and reduces the wavelength of the light pass in through the glass. A parallel beam of light incident at an angle on a polished glass of glass is deflected, and the ratio of the angle of incidence on the surface to the angle of transmission through the glass is determined by the refractive index of the glass as we can see in figure 2.9 [32].



$$m = \frac{\tan(\alpha_i)}{\tan(\alpha_r)}$$
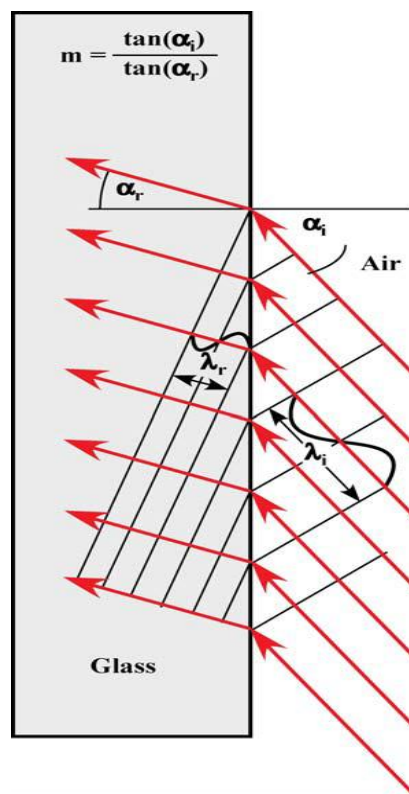
Figure 2.10. Beam of parallel light deflected on entering a block of glass Adapted from [32].

The optical microscope is a sophisticated instrument capable of providing images with a resolution in the order of 1μm, chemical information due to the colour changes or through the use of specific dyes, and, molecular information via birefringence. Combining these factors with a

27

relative ease sample preparation and a low purchase cost, makes the optical microscopy a powerful technique for the study of many materials [36].

In the present work, the transmitted-light microscopy was used. Normally, this technique is used for transparent specimens. Among the various illuminations modes, was used the bright-field illumination. In this mode of illumination, the incident illumination to the specimen surface is on axis with the optic axis through the objective lens, and is normal to the specimen surface [37].

## 2.2.5. Fourier Transform Infrared Spectroscopy (FTIR)

Fourier Transform infrared Spectroscopy analysis it's a conventional way to investigate the miscibility of polymers, by analyzing the shifts of the characteristic bands of the components [38]. As a spectroscopy technique, it allows quantitive determination of composition or binding states through vibracional modes 24]. This technique has the advantage of being almost universal and nearly all kind of samples can have their infrared spectra measured. The spectra provided by this technique is rich in information, easy to use, fast, inexpensive and sensitive [39].

The main component of any FTIR is the Interferometer. This FTIR component splits the single light beam into two light beams. When the two light beams travels their different paths, they are recombined into one beam that leaves the interferometer. Hence, the interferograme yields a single beam spectrum. After the background spectrum is complete, the sample is placed in the infrared beam and the interferograms will be measured with the sample present. These interferograms will be added together and then Fourier transformed in order to obtain the sample single beam spectrum which contain contributions from the environment, the instrument, and the sample [39].

FTIR can be used in three modes, transmission, reflection and attenuated total reflection [28]. In the transmission mode, the sample should present thin section. In the reflection mode, the measurements may lead to a distorced spectra depending on whether the refletion regime is specular or diffuse or, a mixture of both. These problems can be beat by using the attenuated total reflection (ATR) mode; however in this case the surface has to be flat [38,40].

## 2.2.6. Scanning Electron Microscopy (SEM)

The Scanning electron microscope reveals an image of the surface at nanometer lateral resolution where contrast is obtained by electron absorption or emission [28]. The visual impact of scanning electron microscope images and it's ability to reveal details that are displaced along the optic axis, in addition to those resolved in the twodimensional field of view of the image plane, has led SEM to be very used in science and engineering [41].

The Scannning electron microscope (Figure 2.10) comprises a electron gun, two condenser lens, an objective lens, an electron detection system, and a set of deflectors. All these components operate in vacuum [42].
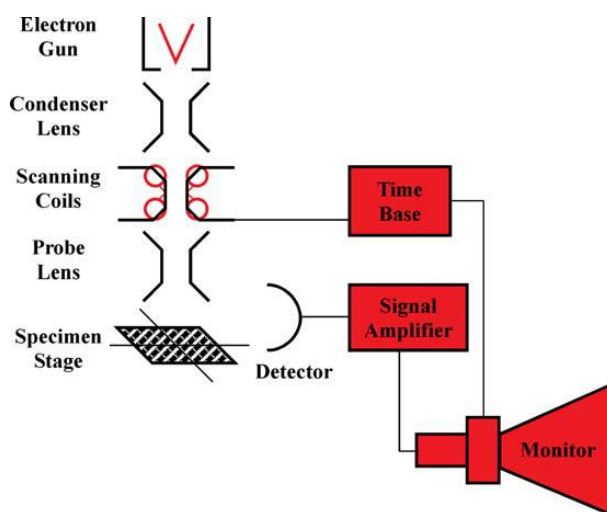


Figure 2.11. Comprising of a scanning electron microscope. Adapted from [28].

The electron gun provides a source of electrons. These are emitted from either a white-hot tungsten or a lanthanum hexaboride [43]. The electrons are accelerated energies ranging from 1to 30 keV. The smallest beam cross-section at the source is subsequently demagnified by the three-stage electron lens system in order to form an electron probe in the surface of the sample. The electron beam emerges from the final lens into the sample chamber wher interactes with the near-surface region of the sample to a depth of approximately 1 μm generating signal electrons used to form an image. The deflection system that is in front of the final lens scans the electron probe in across the sample and operates in synchronism with a computer display monitor, or a

cathode-ray tube. The electron detectors collects signal from the primary beam/specimen interection (Figure 2.11). When the primary beam penetrates the sample surface, it scatters electrons from a variety of different depths, some of which escapes from the surface. These electrons are the secondary electrons and are created by inelastic collisions. Multiple elastic collisions creates backscattered electrons and they are scattered back from deeper levels. This two types of electron make up the most common signals used in SEM images [39,40].
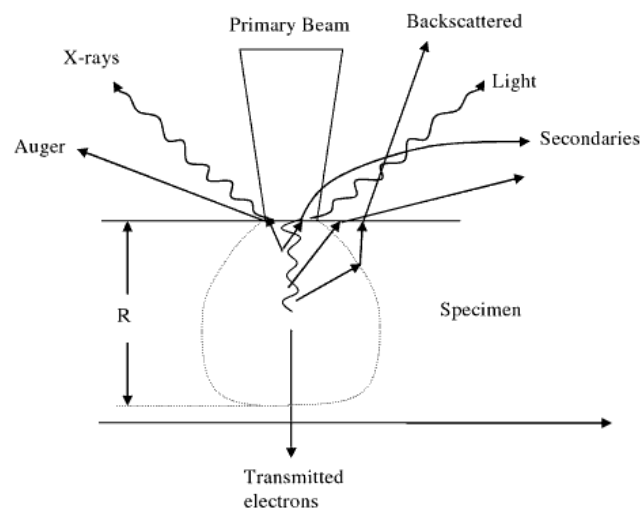


Figure 2.12. Scheme of the Beam/sample interaction . Adapted from [39].

In order to increase the signal in the scanning electron and to obtain an image with a better resolution, the specimens are usually deposited with chromium or gold [37].

## 2.3. References

1. Ravi Kumar, M.N.V., A review of chitin and chitosan applications. Reactive and Functional Polymers, 2000. 46(1): p. 1-27.

2. Kittur, F.S., et al., Characterization of chitin, chitosan and their carboxymethyl derivatives by differential scanning calorimetry. Carbohydrate Polymers, 2002. 49(2): p. 185-193.

3. Tiyaboonchai, W., Chitosan Nanoparticules: A Promising System for Drug Delivery. Naresuan University Journal, 2003. 11(3): p. 51-66

4. Dutta, P.K., J. Dutta, and V.S. Tripathi, Chitin and chitosan: Chemistry, properties and applications. Journal of Scientific & Industrial Research, 2004. 63(1): p. 20-31.

5. Ilium, L., Chitosan and Its Use as a Pharmaceutical Excipient. Pharmaceutical Research, 1998. 15(9): p. 1326-1331.

6. Rinaudo, M., Chitin and chitosan: Properties and applications. Progress in Polymer Science, 2006. 31(7): p. 603-632.

7. Sakurai, K., Maegawa, T., & Takahashi, T. (2000). Glass transition temperature of chitosan and miscibility of chitosan/poly(N-vinyl pyrrolidone) blends. Polymer, 41(19), 7051-7056.

8. Caridade, S.G., et al., Effect of solvent-dependent viscoelastic properties of chitosan membranes on the permeation of low molecular weight drugs. Tissue Engineering Part A, 2008. 14(5): p. 842-842. Shantha, K. L., & Harding, D. R. K. (2002). Synthesis and characterisation of chemically modified chitosan microspheres. Carbohydrate Polymers, 48(3), 247-253.

9. Mucha, M., & Pawlak, A. (2005). Thermal analysis of chitosan and its blends. Thermochimica Acta, 427(1-2), 69-76.

10. Shirosaki, Y., et al., In vitro cytocompatibility of MG63 cells on chitosan-organosiloxane hybrid membranes. Biomaterials, 2005. 26(5): p. 485-493.

11. Inmaculada Aranaz, M.M., Ruth Harris, Inés Paños, Beatriz Miralles, Niuris Acosta, Gemma Galed, Ángeles Heras, Functional Characterization of Chitin and Chitosan. Current Chemical Biology, 2009(3): p. 203-230.

12. Wan, Y., et al., Porous polylactide/chitosan scaffolds for tissue engineering. Journal of Biomedical Materials Research Part A, 2007. 80A(4): p. 776-789.

13. Wan, Y., et al., Mechanical Properties of Porous Polylactide/Chitosan Blend Membranes. Macromolecular Materials and Engineering, 2007. 292(5): p. 598-607.

14. Lehermeier, H.J., J.R. Dorgan, and J.D. Way, Gas permeation properties of poly(lactic acid). Journal of Membrane Science, 2001. 190(2): p. 243-251.

15. Wan, Y., et al., Biodegradable Polylactide/Chitosan Blend Membranes. Biomacromolecules, 2006. 7(4): p. 1362-1372.

16. Alves, N.M., et al., Preparation and Characterization of New Biodegradable Films Made from Poly(L-Lactic Acid) and Chitosan Blends Using a Common Solvent. Journal of Macromolecular Science, Part B, 2011. 50(6): p. 1121-1129.

17. Dechy-Cabaret, O., B. Martin-Vaca, and D. Bourissou, Controlled Ring-Opening Polymerization of Lactide and Glycolide. Chemical Reviews, 2004. 104(12): p. 6147-6176.

18. Lin, Y., et al., Surface modification of poly(l-lactic acid) to improve its cytocompatibility via assembly of polyelectrolytes and gelatin. Acta Biomaterialia, 2006. 2(2): p. 155-164.

19. Gabbott, P., Principles and Applications of Thermal Analysis. 2008: Wiley.

20. Cooper, A., Biophysical Chemistry. 2004: Royal Society of Chemistry.

21. Bershteĭn, V.A. and V.M. Egorov, Differential scanning calorimetry of polymers: physics, chemistry, analysis, technology. 1994: Ellis Horwood.

22. Groenewoud, W.M., Characterisation of Polymers by Thermal Analysis. 2001: Elsevier.

23. Ratner, B.D., A.S. Hoffman, and F.J. Schoen, Biomaterials Science: An Introduction to Materials in Medicine. 2004: Elsevier Science.

24. Höhne, G., W.F. Hemminger, and H.J. Flammersheim, Differential Scanning Calorimetry. 2003: Springer.

25. Menczel, J.D. and R.B. Prime, Thermal Analysis of Polymers, Fundamentals and Applications. 2009: Wiley.

26. Menard, K.P., Dynamic Mechanical Analysis: A Practical Introduction, Second Edition. 2008: Taylor & Francis.

27. Stamm, M., Polymer Surfaces and Interfaces: Characterization, Modification and Applications. 2008: Springer.

28. Erbil, H.Y., Surface Chemistry of Solid and Liquid Interfaces. 2006: John Wiley & Sons.

29. Mittal, K.L., Contact Angle, Wettability and Adhesion. 2009: Brill Academic Pub.

30. Butt, H.J., K. Graf, and M. Kappl, Physics and Chemistry of Interfaces. 2006: Wiley.

31. Brandon, D. and W.D. Kaplan, Microstructural Characterization of Materials. 2008: Wiley.

32. Sheppard, C. and D. Shotton, Confocal laser scanning microscopy. 1997: BIOS Scientific.

33. Pawley, J., Handbook of Biological Confocal Microscopy. 2006: Springer.

34. Murphy, D.B. and M.W. Davidson, Fundamentals of Light Microscopy and Electronic Imaging. 2012: Wiley.

35. Davis, F.J., Polymer Chemistry:A Practical Approach: A Practical Approach. 2004: OUP Oxford.

36. Kaufmann, E.N., Characterization of materials. 2003: Wiley-Interscience.

37. De Giacomo, O., A. Cesàro, and L. Quaroni, Synchrotron Based FTIR Spectromicroscopy of Biopolymer Blends Undergoing Phase Separation. Food Biophysics, 2008. 3(1): p. 77-86.

38. Smith, B.C., Fundamentals of FourierTransform Infrared Spectroscopy, Second Edition. 2009: Taylor & Francis.

39. Vogel, C., E. Wessel, and H.W. Siesler, FT-IR Imaging Spectroscopy of Phase Separation in Blends of Poly(3-hydroxybutyrate) with Poly(l-lactic acid) and Poly(ϵ-caprolactone). Biomacromolecules, 2007. 9(2): p. 523-527.

40. Brandon, D. and W.D. Kaplan, Microstructural Characterization of Materials. 2008: Wiley

41. Khursheed, A., Scanning Electron Microscope Optics and Spectrometers. 2011: World Scientific.

42. Lyman, C.E., Scanning Electron Microscopy, X-Ray Microanalysis, and Analytical Electron Microscopy: A Laboratory Workbook. 1990: Plenum Press.

# Chapter 3: Effect of Composition on Distinct Properties of Biodegradable Blends of Poly-(L-lactic) acid and Chitosan

C. S. Ferreira[1,2], S. G. Caridade[1,2], J. F. Mano[1,2], N.M. Alves[1,2,*]

[1]3B´s Research Group – Biomaterials, Biodegradables and Biomimetics, University of Minho, Headquarters of the European Institute of Excellence on Tissue Engineering and Regenerative Medicine. AvePark, 4806-909, Taipas, Guimarães, Portugal.

[2]ICVS/3B's PT Government Associate Laboratory, Braga|Guimarães, Portugal.

[*] Author for correspondence: 3B´s Research Group – Biomaterials, Biodegradables and Biomimetics, University of Minho, Headquarters of the European Institute of Excellence on Tissue Engineering and Regenerative Medicine. AvePark, 4806-909, Taipas, Guimarães, Portugal. Tel.: +351 253510900; fax: +351 253510909. E-mail address: nalves@dep.uminho.pt (Natália M. Alves).

## Abstract

The present work reports the optimization of a method for the preparation of poly(L-lactic) acid (PLLA) and chitosan (CHT) blends, previously developed at our research group. This simple method is based on the use of a common solvent for the two polymers, hexafluor-2-propanol (HFIP), to produce a homogeneous solution containing PLLA and CHT and the obtention of the films by solvent casting. Films with different fractions of each component were successfully prepared with the optimized method and didn't show visible phase separation. The effect of the blend composition on the wetability and morphology of the films was investigated by contact angle (CA) measurements and scanning electron microscopy (SEM), respectively. Swelling measurements were also conducted on the prepared samples. The influence of the blend composition on their thermal properties and miscibility was analysed by differential scanning

34

calorimetry (DSC). Isothermal crystallization studies were also performed by DSC in order to enhance the comprehension about the effect of the presence of the CHT fraction on the PLLA crystallization process. The miscibility of the films as a function of their composition was evaluated in further detail by optical microscopy (OM) and Fourier transform infrared (FTIR) spectroscopy imaging.

Moreover, the viscoelastic behaviour of the developed PLLA/CHT films was studied for the first time by dynamical mechanical (DMA) in an unconventional way. Namely the mechanical properties of these films were measured while they were immersed in gradient compositions of water/ethanol mixtures. This procedure allowed the analysis of the glass transition dynamics of the CHT fraction, which would not be possible with conventional DMA tests. DMA temperature scans for the samples in the wet state were also conducted.

**Keywords:** polylactides, chitosan, blends, DMA, DSC, FTIR, OM

## 3.1. Introduction

Over the past two decades polymers from renewable resources have been attracted much attention mainly due to environmental concerns and to the petroleum crisis. Generally, these polymers can be divided in two groups, natural polymers and synthetic polymers [1]. Usually, these polymers possess a good processability, dimensional stability and adequate mechanical properties for a large range of applications [2].

Chitosan (CHT) is a natural polymer that can be obtained by alkaline deacetylation of chitin, which after cellulose is the most abundant polymer in nature and is the main component of exoskeletons of crustaceans and cell wall of insects and fungi [3,4]. Chitosan is available in a wide range of degrees of deacetylation and molecular weights [5]. This polymer is known for being non toxic, bioadhesive, biodegradable, biocompatible and presenting antimicrobial activity [4,6]. Due to these properties, CHT has been used in distinct biomedical applications such as tissue engineering, drug delivery systems, artificial skin and burn treatments [3,6].

Poly(L-lactic) acid (PLLA) is a synthetic polymer and its crystallinity, glass transition and melting temperatures can vary in a certain range depending on the polymerization routes and the molecular weight of the resultant product [7]. Due to some of its properties such as biodegradability, biocompatibility and good mechanical properties, PLLA has a wide range of applications on the biomedical field such as sutures, surgical devices, drug delivery and screws for bone fractures, biosensors or ocular inserts [4,8]. However, PLLA has some drawbacks that needed to be improved: the absence of cell recognition sites decreases the cell affinity and adhesion, its hydrophobicity and the acidic degradation products that causes a decline of the pH in the implant zone, which could lead to an inflammatory process [4].

So, when PLLA and CHT are successfully blended, CHT can provide its merits to offset PLLA demerits referred above. Namely, the PLLA/CHT blends should be adhesive and hydrophilic. Other main advantage is that CHT can effectively buffer the acidic degradation products of PLLA due to CHT basicity [4,9]. However it is not easy to blend CHT with polylactides, especially at a highly miscible level although some attempts have been made [10-12]. But the blends prepared in the referred works showed evidences of phase separation [10-12].

In a previous work, we successfully prepared PLLA/CHT films based on the use of a common solvent for the two polymers, hexafluor-2-propanol (HFIP), which didn't show visible phase separation [9]. In the present work, the method of preparation was modified, as explained at the experimental section, in order to simplify it and to try to improve blend miscibility. Also, only a preliminary characterization of the PLLA/CHT films was performed by DSC in the previous work [9]. In this work a quite complete characterization of several properties of the films prepared by this simpler method was performed by the first time. Namely, wetability, morphology, swelling, thermal properties (glass transition, melting and crystallization behavior), miscibility and mechanical/viscoelastic properties were analysed as a function of the film composition.

Moreover, DMA temperature scans of the PLLA/CHT blends in the wet state were also performed. In particular, the viscoelastic properties of the films were measured by dynamic mechanical analysis (DMA) with the samples immersed in a bath containing a water/ethanol mixture. Such non-conventional methodology can be useful to explore the materials behavior in

more realistic conditions, relatively to their applications, and to extract relevant information about the dynamic behavior of materials under different liquid environments [13].

## 3.2 Experimental

### 3.2.1. Materials

Chitosan (medium molecular weight and degree of N-deacetylation of 80%) was purchased from Sigma-Aldrich. Poly(L-lactic) acid (low molecular weight) was purchased from Purac. Hexafluor-2-propanol (HFIP) was obtained from Aldrich.

### 3.2.2. Preparation of PLLA/CHT blends

PLLA/CHT films were prepared by solvent casting. First, two solutions of both polymers were prepared under stirring, a 2% w/v of PLLA in HFIP and a 0,5% w/v solution of CHT in HFIP. Then, the PLLA/HFIP solution was slowly added to the CHT/HFIP solution under vigorous stirring for each prepared condition (PLLA75_CHT25, PLLA50_CHT50, and PLLA25_CHT75). The blended solutions were kept in a chemical wood for three days in order to evaporate the liquid phase. Afterwards, the films were extensively washed with ethanol and then with distilled water to remove the solvent residues. Finally, the films were dried at $50^{0}C$ in the vacuum oven for one week to completely remove the solvents. Two control films of pure PLLA and pure CHT were also prepared using the same method. So, the step that involved the use of methanol to precipitate the films used in the procedure previously proposed by us [9] was eliminated.

### 3.2.3. Contact Angles Measurement

The contact angle measurements were obtained by the sessile drop method using a contact angle meter OCA15+ with a high-performance image processing system (DataPhysics Instruments, Germany). The liquid (water) was added by a motor-driven syringe at room temperature. Five measurements were carried out for each sample.

### 3.2.4. Scanning Electron Microscopy (SEM)

A Leica Cambridge S360 microscope was used in order to analyse the morphology of the PLLA/CHT films. All the samples were sputtered coated with gold and the analysis were performed at an accelerating voltage of 10 kV with magnifications between 50 - 2000 times.

### 3.2.5. Swelling

The swelling of PLLA/CHT films was measured in water/ethanol mixtures and not only in water, as typical, in order to correlate these results with the unconventional DMA results that were performed under the same solvent mixtures. The swelling of PLLA/CHT films in water/ethanol mixtures was determined by immersing previously the weighted films in mixtures of water ethanol at compositions varying from pure water to pure ethanol, after around 10min to 24h, swollen samples were blotted with filter paper to remove the solvent excesses and weighted immediately. The swelling ratio (S) was calculated using the following equation:

$$S\left(\text{wt.}\%\right)=\frac{W-W_0}{W_0}\times100 \tag{1}$$

Where $W_0$ is the initial weight of the sample and w the weight of the swollen sample.

### 3.2.6. Differential Scanning Calorimetry (DSC)

The DSC analyses were carried out in a DSC Q100 V9.8 from TA Instruments, calibrated with an indium standard under nitrogen atmosphere. The samples were heated until the melting of the PLLA component and then quenched to $10°C$. Then, the scans were performed from $10°C$ to $200°C$ at a rate of $20°C/min$. For the isothermal cold crystallization experiments, the PLLA/CHT membranes were heated until $200°C$ and kept at this temperature for three minutes. Then, the samples were cooled to a defined crystallization temperature $T_c$ at a rate of $80°C/min$ and held there for 60 minutes. The crystallization behavior of PLLA and PLLA/CHT blends was analysed by DSC at various $T_c$. In the case of pure PLLA, the selected $T_c$ were 95, 105, 110, 115, 120, 125, 130, 135 and 140°C. Two $T_c$ were chosen for the PLLA/CHT blends: 105 and 110°C.

### 3.2.7. Optical Microscopy (OM)

Samples were cut with about 10mm of length and 10mm of width. The average films thickness was 2 μm. The PLLA/CHT samples were stained with eosin, which specifically stains the CHT component of the films. The stained films were observed in a light microscope (Zeiss Imager Z1m microscope).

### 3.2.8. Fourier Transform Infrared (FTIR) spectroscopic Imaging Measurements

The FTIR image measurements were performed using the Perkin Elmer Spotlight 300 FTIR Microscope System. In order to construct FTIR maps, spectra were collected in the continuous scan mode. PLLA and CHT characteristic maps were centered at a1759 and 1565 cm$^{-1}$ respectively. The PLLA/CHT images were mapped for a sample areas of 1000 X 1000 μm$^2$ with a spectral resolution of 25 cm$^{-1}$.

### 3.2.9. Dynamical Mechanical Analysis (DMA)

The DMA analyses were carried out in a TRITEC200B DMA from Triton Technology (UK) equipped with the tensile mode. The distance between the clamps was 5mm and the PLLA/CHT films were cut with about 20mm of length and 4mm of width. The average film thickness was 2μm. Before each experiment, the geometry of each film was accurately measured. The films were tested at a constant frequency (1 and 5 Hz) and the experiments were performed under constant strain amplitude of 30 μm. During the tests a pre load of 0.1N was applied in order to keep the films tight. The experiments were repeated three times for the distinct samples and were extremely reproducible. First, temperature scans at a heating rate of 1 °C/min between 20°C and 70 °C were performed, in order to study the variation of $E'$ and tan $\delta$ of the films in the glass transition region of PLLA.

For the unconventional DMA tests, after measuring the film geometry, the samples were clamped in the DMA apparatus and immersed in a recipient with 450ml of ethanol. The measurements were carried out at room temperature (20°C). During the tests, the changes of the storage modulus ($E'$) and the damping factor (tan $\delta$) as a function of the water content were monitored. $E'$ increases until an equilibrium value where changes were no longer detected, the water was pumped into the reservoir at a constant flow rate ($Q$), providing a time dependent change in the

content of water that can be described by the following equation where $V_{EtOH}$ is the ethanol volume:

$$water\,(vol.\%) = \frac{Qt}{Qt + V_{EtOH}} \tag{2}$$

These unconventional DMA tests were performed with the intention of analyzing the viscoelastic behaviour of the CHT component, which is very difficult to achieve with conventional DMA tests.

## 3.3. Results and Discussion

### 3.3.1. Contact Angle Results

By using the optimized procedure described at the experimental part, three blends were successfully produced and designated as PLLA50_CHT50, PLLA75_CHT25, and PLLA25_CHT75, where the numbers represent the mass percentages of CHT and PLLA in the blend. All the films appeared homogeneous, with no evident macroscopic phase separation, similarly to what was found for the films prepared with the previous procedure [9]. Contact angle measurements were performed with the prepared films in order to analyse if the blend composition affects their wettability. Other authors have analysed the effect of blend composition on the wetability of PLLA/CHT blends [4,14]. Wan et co-workers [4] measured the water contact angles of PLLA/CHT blends and they concluded that, as the CHT content in the blends increased the contact angle decreased. Yuan et al [14] prepared CHT-g-PLLA copolymers and also found a decrease in the water contact angle, concluding that grafting PLLA onto CHT improves the PLLA hydrophilicity. The results for the PLLA/CHT blends prepared in this work are shown in Figure 3.1. It can be seen that the contact angle decreased approximately from 90 to 78°C, for the blends, i.e., the wetability increased as the CHT content increased, in agreement with the referred works [4,14]. Also, the contact angles of the control samples (PLLA and CHT pure films) are almost the same, nearly ≈80°, which was an unexpected result. So, probably there are other factors such as different film morphology as a function of composition, besides the effect of adding a polymer with higher hydophilicity to PLLA, which might explain this unexpected result. Regarding the potential use of these blends in biomedical applications, it has been reported that

optimal cell adhesion occurred for polymer surfaces presenting moderate wettability [15,16]. although it is also true that cell adhesion and differentiation is quite dependent not only on wettability but on other factors such as surface topography, chemistry and, in particular, cell type [17].
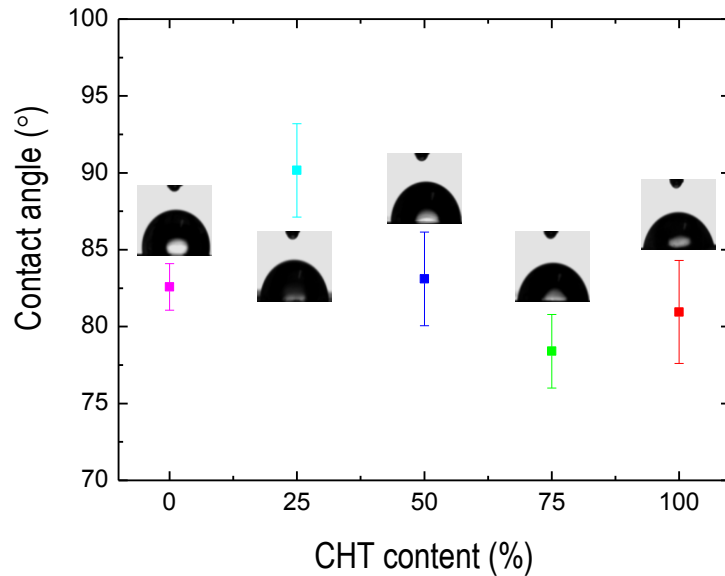


Figure 3.1. Contact angle measurements of PLLA/CHT films.

## 3.3.2. SEM Results

SEM analysis was conducted in order to investigate the morphology of the prepared samples as a function of composition - Figure 3.2. It can be seen that, .in fact, film morphology is different as a function of composition. PLLA (Figure 3.2 (a)) presents a smooth surface with some pores whereas CHT (Figure 3.2 (b)) exhibited a smooth surface without pores These features explain the similar contact angles values of PLLA and CHT films mentioned above. Also, all the PLLA/CHT blends (Figures 3.2 (c, d, e)) present a rough surface without pores, however the roughness is somewhat different depending on the composition, for example, it seems that PLLA50_CHT50 surface is rougher than the surfaces of the other blends. So, the distinct morphology of the films as a function of composition could explain the contact angle results, as previously suggested,

Wan et al [7] have produced porous PLLA/CHT films and found that their porosity decreased with increasing CHT content. Whereas Lim et al [18] have fabricated PLLA/CHT

scaffolds and observed that their that porosity increased with increasing CHT ratio. So, it seems that the porosity of PLLA/CHT blends is affected by the CHT content and of course, on the preparation method [7,18]. In our case, it was not the purpose to obtain porous materials, i.e, a porogen agent was not used, for instance, but in fact the use of this particular method with PLLA, allowed to obtain porous PLLA samples.
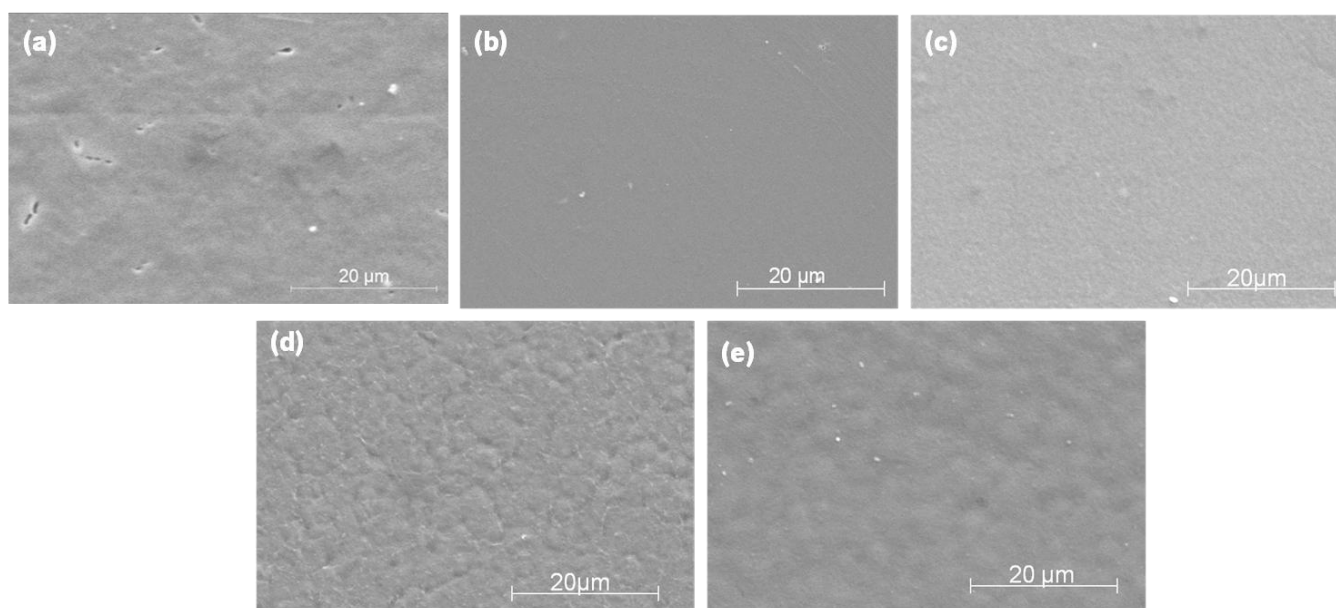


Figure 3.2. SEM images of PLLA/CHT films. (a) pure PLLA, (b) pure CHT, (c) PLLA25_CHT75, (d) PLLA50_CHT50, (e) PLLA75_CHT25

### 3.3.3. Swelling Results

Semi-crystalline polymers, in the presence of suitable solvents absorb limited amounts of solvent swelling until the equilibrium is reached. When combining the effect of a solvent with a non-solvent, is expected to be rather useful to control the swelling ratio within polymers. CHT absorbs considerable amounts of water when immersed in aqueous environments [13]. PLLA is a hydrophobic polymer [7], for this reason, it isn't expected to absorb water. For the water/ethanol mixtures, the equilibrium swelling ratio was considered to have been achieved after 6h, due to the fact that the swelling ratio between 6 and 24h did not show significant differences (please see annex 1).

Figure 3.3 shows the dependence on the ethanol content of the swelling ratio of the PLLA/CHT films. As expected, the films with the highest amount of CHT presented a higher swelling ratio. The increasing ethanol content in the water/ethanol mixtures decreased the swelling ratio. The pure PLLA film presented a swelling ratio much higher than expected for a hydrophobic polymer. This fact can be explained by the fact that the PLLA films present pores as the SEM image presented in Figure 3.2. (a) showed. Suytma et al [19] prepared PLLA/CHT films and they concluded that the increase of the PLLA components decreases the water sensitivity of CHT. These results are in agreement with the ones found in the present work. Da Silva et al [20] immersed CHT membranes in isopropanol/water mixtures and they found that the swelling equilibrium degree decreases progressively with the increasing content of isopropanol. Caridade et al [13] studied the swelling behavior of CHT membranes in water/ethanol mixtures and it was concluded that the increasing content of ethanol on the ethanol/water mixtures decreases the membranes swelling capability. We also observed a decrease in the swelling capability as the alcohol content in the mixture increased for all the prepared samples, independently of their composition (Figure 3.3).



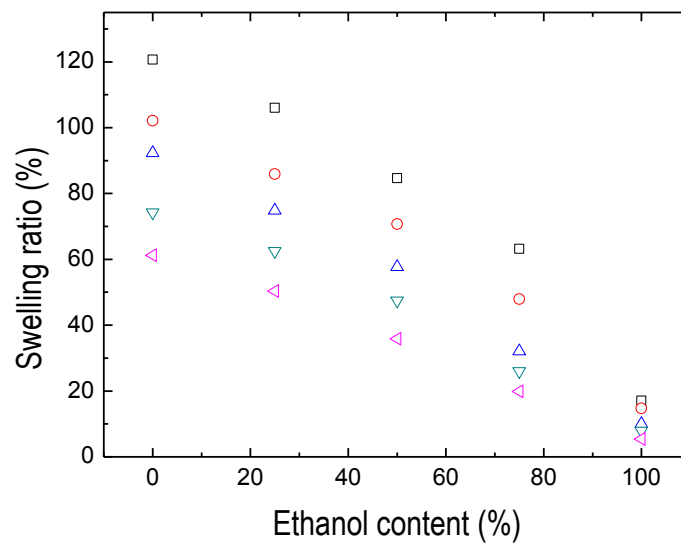Figure 3.3. Dependence of the ethanol content of the equilibrium swelling ratio ($S_{eq}$) determinate after immersion in water/ethanol mixtures for PLLA/CHT films for 24h.[CHT ( □ ), PLLA25_CHT75 ( ○ ), PLLA50_CHT50 (△), PLLA75_CHT25 (▽), PLLA(◁ )]

### 3.3.4. DSC Results

DSC experiments were performed in order to obtain information about the thermal properties of the blended films and also to get some insights about their miscibility. Glass transition temperature ($T_g$) is a property that could be used to evaluate the miscibility of two components of a blend. If the two components were completely miscible, the DSC data of the blend would only show one $T_g$ whose value is among the values of the pure components of the blend [4]; if the two components were partially miscible, the blend would present two temperatures that are related with which one of the blend components [4].

The DSC scans of PLLA, PLLA75_CHT25, PLLA50_CHT 50 and PLLA25_CHT75 prepared with the optimized method described at the experimental section are shown in Figure 3.4 and the characteristic temperatures are summarized in Table 3.1. It is well known that the thermal properties of CHT are very difficult to observed by DSC [21-23]. So, only the thermal events associated to the PLLA fraction, i.e., glass transition, cold crystallization, and melting were clearly visible by DSC for all the compositions in Figure 3.4.

The obtained $T_g$ for pure PLLA was ≈62°C, and when the CHT mass in the membrane increases, the $T_g$ slightly decreases. Although the exact value of the $T_g$ of CHT is not known, it is known that it is above the $T_g$ of PLLA [9,24]. Hence, if the components of the films were partially miscible, the $T_g$ of the blends should increase with the increasing content of CHT, which was not observed in our case. Wan and co-workers [4] have prepared PLLA/CHT blends and they observed a slight increase of $T_g$ with the increase content of CHT. On the other hand, Chen et al [11] have found no changes in the $T_g$ value of PLLA/CHT blends. The slight decrease in $T_g$ observed in our work could be probably due to distinct factors such as the plasticizing effect of residual solvents that could be still present in the samples or, as it is such a small variation, could even be attributed to experimental errors. It could also suggest the presence of some microscopic phase separation, although further investigation about the misciblity of the blends should be conducted to clarify this issue.

Regarding the cold crystallization peak, it can be said that both crystallization temperature and enthalpy decrease with the increasing content of CHT in the blends. This decrease could occur because CHT has rigid chains that interfere with the PLLA chains reorganization, almost preventing cold crystallization when the CHT fraction is equal or above

50%. Chen et al [11] have also observed a decrease in the $T_c$ of their PLLA/CHT blends with increasing CHT content.

The $T_m$ of pure PLLA was ~173°C and this value decreased with the increase of the CHT fraction in the films. This happens probably because less perfect crystalline structures or thinner lamellae were formed when crystallization occurs at lower temperatures, as the CHT fraction increases. Liao et al [25] have prepared O-lauroyl chitosan (OCS)/PLLA blends and have also found that the $T_m$ of the blends decreased with increasing content of OCS.

From the DSC results, it was also possible to calculate the crystallinity degree ($X_c$) of the PLLA fraction by the following equation:

$$X_c = \frac{\Delta H_m - \Delta H_c}{\Delta H_u^0 w} \tag{3}$$

Where $\Delta H_m$ is the melting enthalpy, $\Delta H_u^0$ is the melting enthalpy of fully crystalline PLLA (93 J/g) [9], and $w$ is the mass fraction of PLLA in the blends. The crystallinity values presented in Table 3.1 showed that $X_c$ suffer a pronounced decrease from ≈10% to ≈3% with the increasing content of CHT, So, the PLLA phase in the blends prepared by the optimized method was essentially in the amorphous state. Other authors have observed a decrease in the crystallinity of PLLA/CHT blends prepared by other methodologies [11,18], although in none of these works was an almost suppressed crystallinity of the PLLA component reported when the blends had a CHT fraction equal or higher than 50%.

By comparing the DSC results of the present work with the DSC data obtained with the samples prepared by the previous method [9]. it can be seen that the results are very similar (for further information, please see annex I). So, it can be concluded that the use of methanol to precipitate the samples has no effect on the thermal properties of these PLLA/CHT blended films.
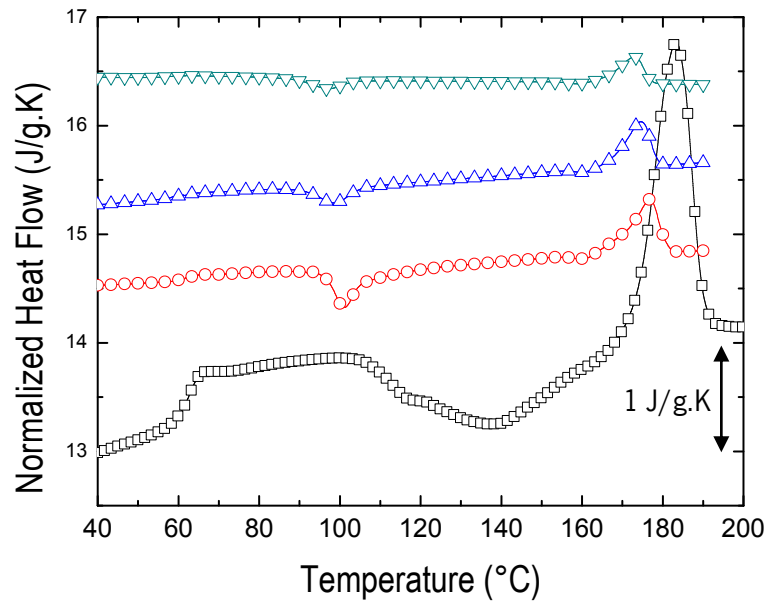
Figure 3.4. DSC thermogram of PLLA/CHT films. [ PLLA ( ─▢─ ), PLLA75_CHT25( ─○─ ), PLLA50_CHT50 ( ─△─), PLLA25_CHT75 ( ─▽─ )]

Table 3.1. Thermal properties of PLLA/CHT films.

|  | $T_g$ (°C) | $T_m$ (°C) | $\Delta H_m$ (J/g) | $T_c$ ($^0$C) | $\Delta H_c$ (J/g) | $X_c$ (%) |
|---|---|---|---|---|---|---|
| **PLLA** | 62.7 | 173.2 | 30.7 | 120.4 | 21.5 | 9.9 |
| **PLLA75_CHT25** | 61.6 | 166.8 | 16.3 | 96.8 | 10.8 | 7.9 |
| **PLLA50_CHT50** | 58.5 | 165.7 | 12.6 | 90.1 | 10.7 | 4.1 |
| **PLLA25_CHT75** | 54.7 | 164.5 | 2.8 | 89.3 | 2.1 | 3 |

The isothermal crystallization behavior of the PLLA/CHT films was also studied by DSC. First, an analysis of the isothermal crystallization behavior of pure PLLA was performed - Figure 3.5. The isothermal crystallization of pure PLLA was not analysed for temperatures lower than 95°C and higher than 140°C due to the fact that it is known from literature that the exothermal heat flow in the PLLA crystallization process is too small to detect by DSC at these temperature ranges [26]. Tthe crystallization rate increased from 95°C to 110°C, as can be seen in Figure

3.4, reaching a maximum at this temperature. Above 110 °C, the crystallization rate decreased. These results are in agreement with the ones found by Yasuniwa et al [26] and by Wu et al [27] The change in the crystallization kinetics of these PLLA films at around 110 °C could be related to a transition of the crystallization regime from III to II. Regime II type occurs when the nucleation rate, i, is high and it spreads slowly at the velocity g, and multiple nucleations take place before the completion of one layer. Regime III type is a case where the nucleation rate, i, is much higher than the velocity, g [28]. The crystallization half-time is defined as the time between the onset of the crystallization and the point where crystallization is 50% complete. This time has been usually used in crystallization kinetic analysis as a overall rate of crystallization [26]. The crystallization half-time of pure PLLA is shown in Figure 3.6. From Figure 3.6 it can be seen that the crystallization half-time decreased from 95°C to 110°C, until it reaches a minimum at this temperature and then it increases again for higher temperatures. This minimum is the temperature where the crystallization peak is more intense, in agreement with the results of Figure 3.5
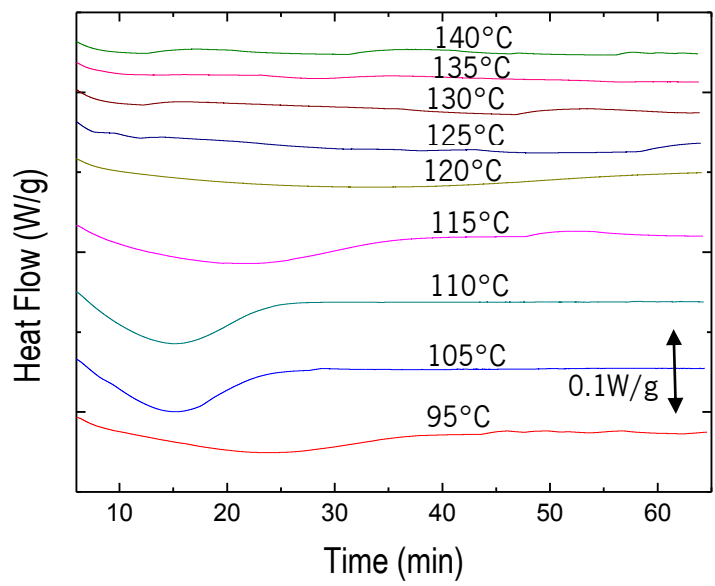


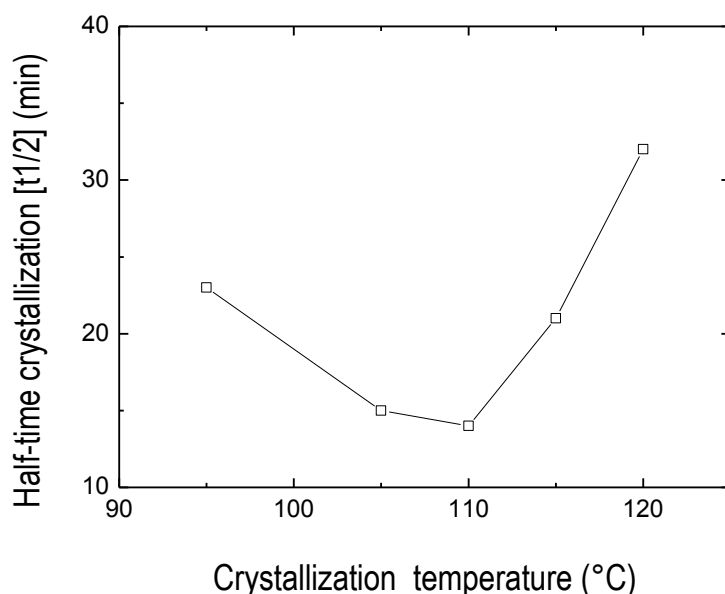Figure 3.5. Crystallization curves of pure PLLA.

Figure 3. 6. Crystallization temperature dependence of the peak crystallization time of pure PLLA film.

The isothermal crystallization curves of PLLA/CHT films were carried out at two temperatures, 105 and 110°C, because these were the temperatures where the isothermal crystallization peaks of pure PLLA were more intense (Figure 3.6). The isothermal crystallization results of PLLA/CHT blends as a function of composition are shown in Figure 3.7. The crystallization peaks are not visible in the curves of this figure, for any of the blends. However, in the DSC curves of Figure 3.7 the PLLA/CHT films present a visible cold crystallization peak for the blend with 25% of CHT and weak crystallizations peaks for the two other compositions. Hence, it cannot be said that the CHT component of the films, at least for the blend with 25% of CHT suppress PLLA crystallization. Therefore, it can be suggested that, for the blends, the isothermal crystallization occurs too fast and/or it is a process with such a low intensity that cannot be detected by DSC isothermal measurements. It should be pointed that, although there are other studies involving isothermal crystallization studies of other PLLA blended films (e.g [8,29] ]) to the best of our knowledge, the isothermal crystallization behavior of PLLA/CHT blended films was never studied until now.
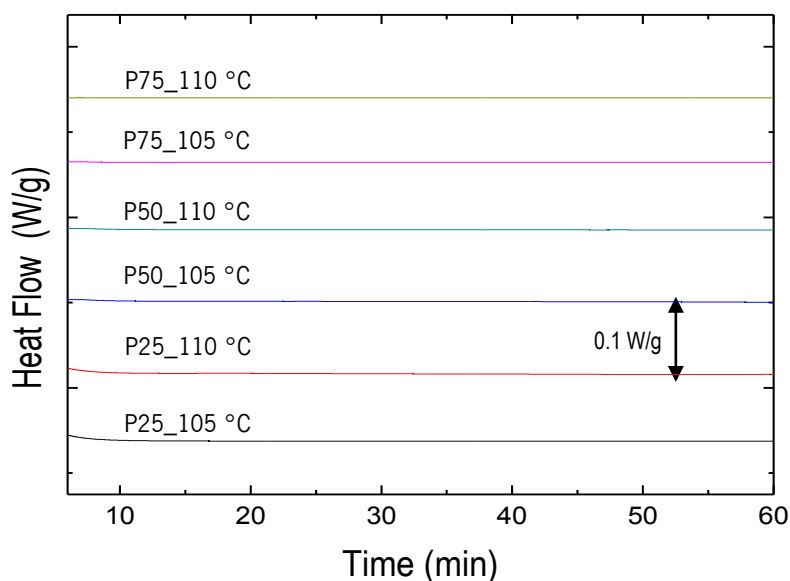
Figure 3.7. Crystallization curve of PLLA/CHT films.

### 3.3.5. Optical Microscopy (OM) Results

Optical Microscopy was performed in order to get more insights about the miscibility of the PLLA/CHT films, as the DSC data were not conclusive. The films were stained with eosin in order to mark the CHT component of the blends. Eosin is a water-soluble ammoniac dye that binds to the amino group of CHT in the protonated state. Hence, CHT was stained by the ion interaction between the anion in the dye and the cation in the polymer [18]. As can be seen in Figure 3.8, the CHT component of the films was successfully marked with eosin, as evidenced by the characteristic pink colour of this stain in the images corresponding to the blends and pure CHT. The staining intensity increased as the CHT fraction increased, as expected. The images also evidenced that there wasn´t a clear phase separation between the two components of the films as the stain is quite homogenous along the samples, independently of the blend composition. So, these results suggested that the miscibility at the microscopic level was very good for all the blend compositions. Lim et al [18] produced CHT/PLLA scaffolds and also marked CHT with eosin, observing a dispersion of the CHT fraction on these scaffolds.
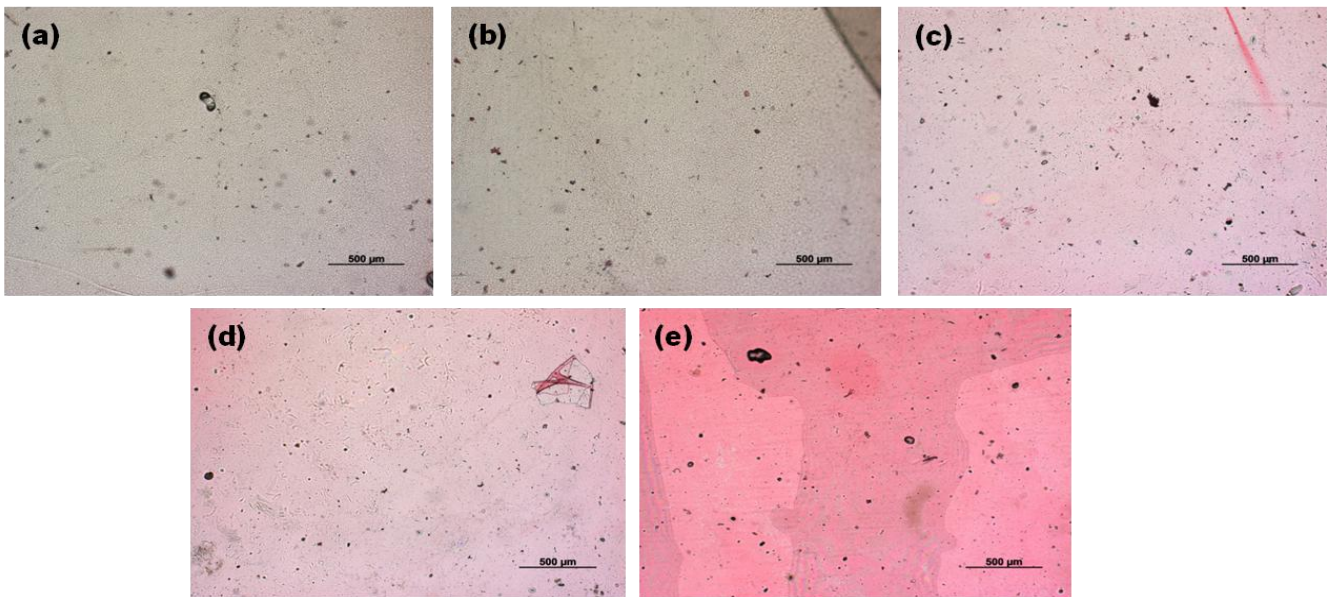
Figure 3.8. Optical microscope images of PLLA/CHT films using eosin dye. (a) pure PLLA, (b) PLLA75_CHT25, (c) PLLA50_CHT50, (d) PLLA25_CHT75, (e) pure CHT (scale bar=500μm).

## 3.3.6. Fourier Tranform Infrared (FTIR) spectroscopic Imaging Results

FTIR imaging analysis was conducted in order to further evaluate the miscibility of the films and complement OM results. False colors were used to identify the two components of the films, red for PLLA and yellow for CHT. FTIR images for PLLA, CHT and the blended films were mapped for 1000x1000 $\mu m^2$ area in the absorbance mode-Figure 3.9. This figure shows that the PLLA/CHT blends present a predominant orange color, which indicates a quite good distribution of both components for all the blends. Therefore, it can be said that there is no microscopic phase separation, of course within the resolution mode of this technique.
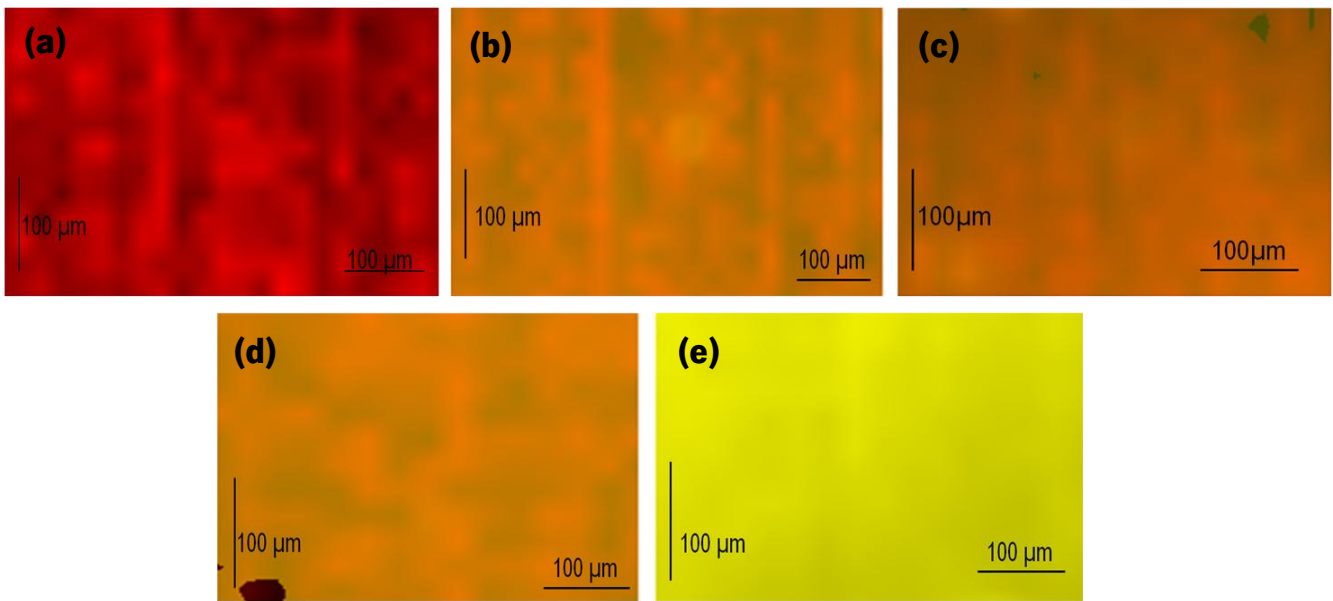
Figure 3.9. Chemical maps of the PLLA/CHT films. (a) pure PLLA, (b) PLLA75_CHT25, (c) PLLA50_CHT50, (d) PLLA25_CHT75, (e) pure CHT.

### 3.3.7. DMA Results

DMA is an adequate technique to characterize the mechanical/viscoelastic properties of a material in a wide temperature range and at several frequencies [13]. It is possible to measure two important properties of the material, the storage modulus ($E'$) and the damping factor (tan δ). $E'$ is a measure of the material hardness and of the energy elastically stored during the process of deformation [30]. Tan δ is a measure of the energy dissipated during the deformation process [4]. $T_g$ is typically measured by DMA as the temperature corresponding to the maximum of the tan δ peak.

Figure 3.10 displays $E'$ (a) and tan δ (b) variation for the films as a function of the temperature and at 1 Hz, respectively. It was not possible to perform these experiments for PLLA25_CHT75 because it was very fragile and these samples broken when the pre-load was applied at the beginning of the experiment. These experiments were performed with the samples immersed in PBS. It can be seen that $E'$ increased with the increasing content of PLLA in the films as expected (Figure 3.10 (a)), because the fraction of the hydrophobic component of the blend increased. It should be pointed that although some DMA temperature scans of CHT based blends can be found in literature [4,31] these experiments are typically performed with the

51

samples in the dry state, originating distinct $E'$ variations as a function of PLLA content than the one found in the present work. It should be stressed that, as already mentioned, CHT is a hydrophilic polymer that can uptake up to 160% of water by weight in simulated physiological conditions, which strongly influence its mechanical properties [13,32].

So, when biomedical or even environmental applications are envisioned for CHT based blends, it is extremely important to analyse the mechanical properties in the wet state, as performed in the present work, in order to simulate their behaviour in a real situation

Regarding tan δ data (Figure 3.10 (b)), the temperature of the maximum of PLLA tan δ was observed at around 80°C, whereas for PLLA75_CHT25 this maximum decreased to around 53°C and for PLLA50_CHT50 this value is around 50°C. This decrease in the temperature of the maximum of tan δ, which is a measure of PLLA $T_g$, could be explained by a plasticizer effect due to the absorption of water by the CHT fraction. It could also be observed that the presence of CHT increased tan δ intensity when compared with the one of the PLLA control films.

The influence of frequency on the dynamic mechanical properties of the PLLA/CHT films was also studied (please see Annex I). The temperature of the maximum of tan δ and E' increased with the increase of frequency. This happens because when the frequency increased the number of cycles of deformation that the sample suffers increased and the time that the polymeric chains have to reorganize themselves decreased.

The variation of $E'$ and tan δ for the films prepared with the previous method [9] was compared with the results of Figure 3.10. It was found that these results are quite similar to the ones shown in Figure 3.10 (please see annex I).
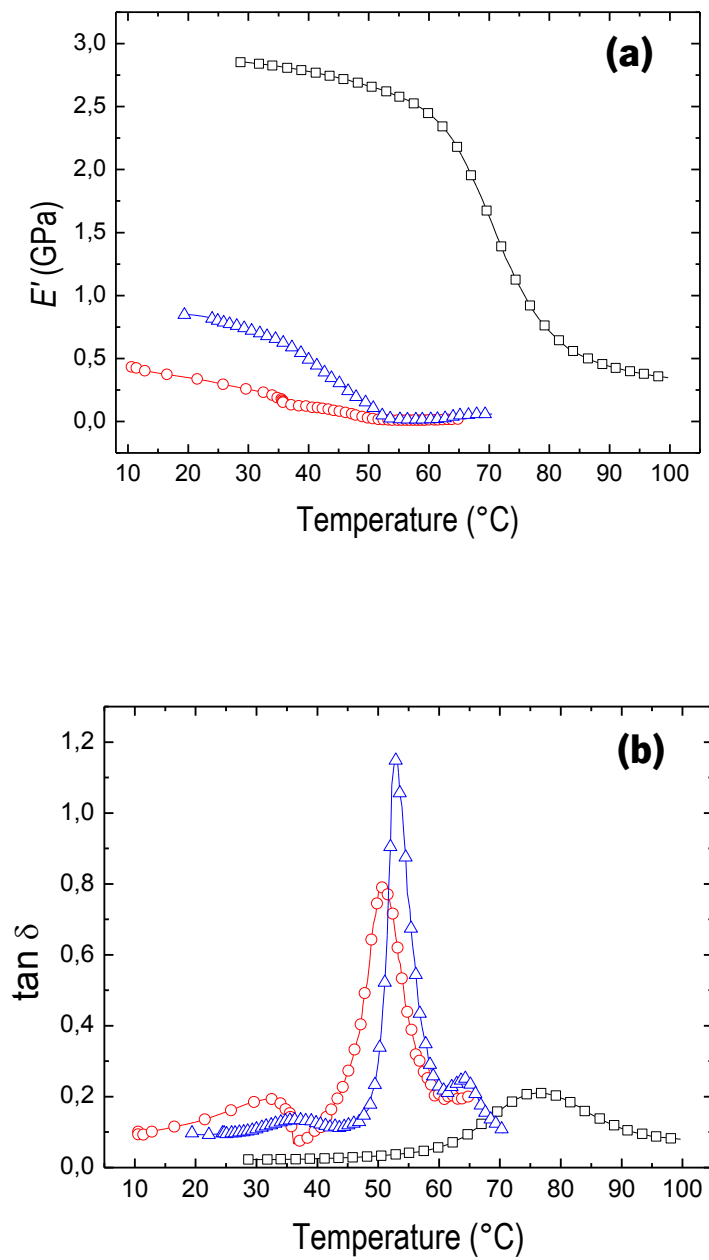
Figure 3.10. Storage modulus (E') (a) and damping factor (tan δ) (b) as a function of temperature of PLLA/CHT films. [PLLA ( ☐ ), PLLA75_CHT25 (△), PLLA50_CHT50 (◯)].

In the present work, DMA experiments were also performed in order to see if the presence of water in the liquid where the samples were immersed during the tests affects the glass transition of the prepared samples. During these tests, the films were clamped in the DMA apparatus and immersed in an ethanol solution and the water was introduced in the reservoir at

53

a constant flow rate, changing the mixture composition. In particular, this procedure allowed to analyse the viscoelastic behavior of the CHT fraction of the blended films. In fact, Caridade et al [13] performed similar experiments only with CHT crosslinked membranes and, when the water content was increased, it was simultaneously observed a peak in the loss factor (around 25 vol.%) and a reduction of the storage modulus, which was attributed to the α-relaxation of CHT. This was the first time that the glass transition dynamics in a polymer was monitored in immersion conditions where the composition of the plasticizer in the bath is changed in a controlled way [13]. So, the change in the composition of water in a water/ethanol mixture could be useful to detect the relaxational process associated to the glass transition. It should be pointed that although the glass transition process in CHT has been addressed in different works [24,33-36], the results are far from being in agreement. In fact, it is not straightforward to detect the glass transition of CHT because is a semi-crystalline biopolymer composed by very stiff chains, that could even form liquid crystalline structures in certain conditions [23].

The results of such unconventional DMA tests for the blends prepared in this work are shown in Figure 3.11. These experiments were also conducted for the pure CHT films, for the sake of comparison (Figure 3.11). So, the tan δ peak detected for pure CHT and for blends (Figure 3.11 (b)) could be assigned to the glass transition phenomenon observed before in CHT membranes adopting a similar strategy [13].

In our case, the peak for pure CHT was observed at about 37 vol.%. For the blends a shift towards lower water content could be observed, from 26% to 20% when the PLLA content increased form 25% to 50%. So, it could be suggested that in this particular case PLLA acts as a plasticizer, enhancing the flexibility of the CHT chains, shifting the peak towards lower water contents. It could also be hypothesized that the presence of PLLA could affect the CHT crystallization kinetics, diminishing its crystallinity degree, which could also help explain the shift in $T_g$ to lower water fractions.

It can also be seen that $E´$ decreased with the increase of the water content in the mixtures, as expected (Figure 3.11 (a)). This figure also evidenced a relationship between the PLLA content of the blends and $E'$. There is an increase of $E'$ with the increase of PLLA content in the blends at the beginning of the experiment, when the sample was only immersed in ethanol. At this point, i.e., at the beginning of the experiment, this would correspond to the situation where the samples are dehydrated. So, as CHT in the dry state is a very stiff polymer [36], an opposite variation should be expected. The trend observed in this particular work could

be attributed to the distinct morphology of the samples, as already mentioned before, in particular to the pores exhibited by the PLLA films (Figure 3.1 (a)).

The influence of frequency on tan δ were also studied in these unconventional DMS tests (please see annex I). E' tended to increases with increasing frequency. Moreover, the tan δ peak shifted to higher contents of water when the frequency increases.
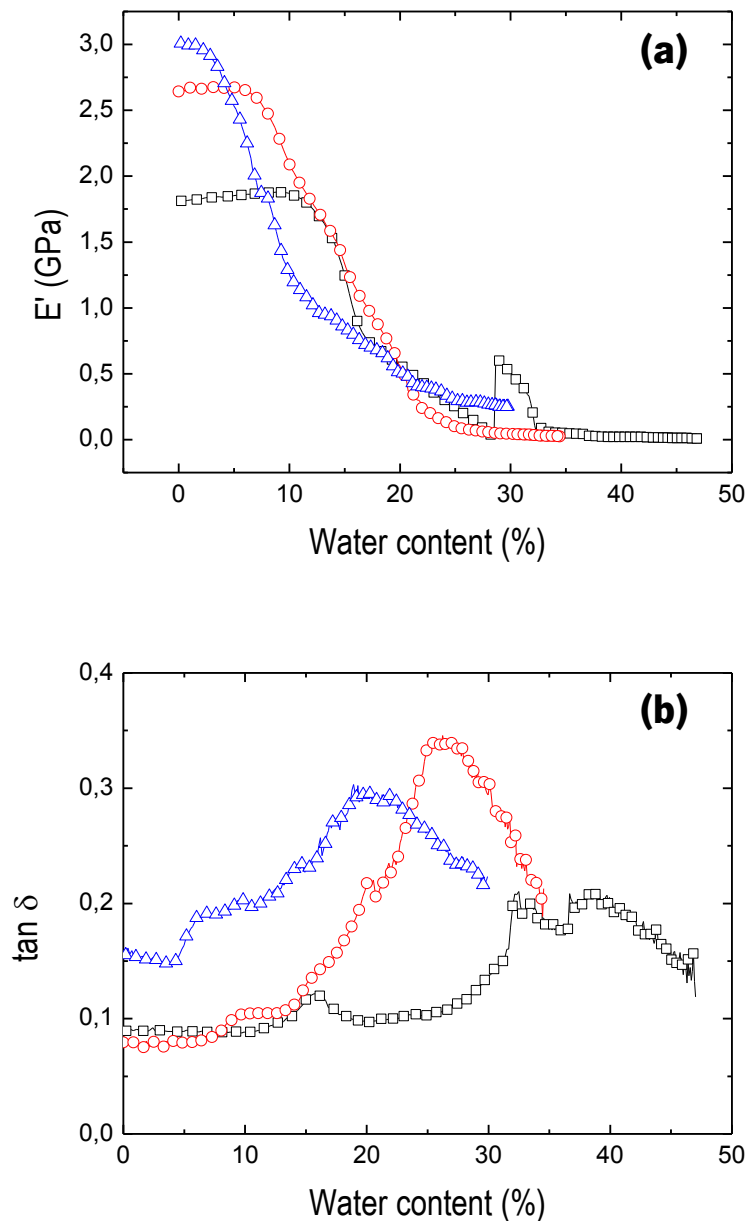


Figure 3.11. Apparent storage modulus (*E'*) (a) and damping factor (tan δ) at room temperature measured with samples immersed in water/ethanol mixtures as a function of water content of PLLA/CHT films. [CHT (—☐—), PLLA25_CHT75 ( —○— ), PLLA50_CHT50 ( —△— )]

## 3.4. Conclusions

Biodegradable blended films of PLLA and CHT with a wide compositional range were successfully prepared by a simple procedure, and didn't present visible phase separation. FTIR and OM analysis evidenced that the blends also presented a good miscibility at the microscopic level, for all the studied compositions.

It was found that the wetability of the blends increased as the CHT content increased and that all presented a rough surface, somewhat different depending on the composition, being PLLA50 CHT50 rougher than the other blends. Regarding swelling, the films with the highest amount of CHT presented a higher swelling ratio.

DSC showed that the presence of CHT in the blends affected significantly both the cold crystallization and isothermal crystallization behaviour of the PLLA fraction, almost preventing crystallization when the CHT fraction is equal or above 50%.

Temperature DMA results allowed to conclude that E' increased as the PLLA content in the blends increased and that the $T_g$ of PLLA decreased when the CHT fraction increased, probably to a plasticizer effect. Tan δ is also higher for the blends than for the PLLA control films, due to the presence of CHT.

Unconventional DMA tests allowed to analyse the glass transition process of the CHT fraction of the blends. A shift of the $T_g$ of the CHT fraction towards lower water content was found, from 26% to 20% when the PLLA content increased from 25% to 50.% It was also possible to conclude that the storage modulus of the blends decreased with the increase of water content.

.

## 3.5. Acknowledgments

## 3.6. References

1. Yu, L., K. Dean, and L. Li, *Polymer blends and composites from renewable resources.* Progress in Polymer Science, 2006. 31(6): p. 576-602.

2. Zeng, J.B., et al., *Miscibility and Crystallization Behaviors of Poly(butylene succinate) and Poly(L-lactic acid) Segments in Their Multiblock Copoly(ester urethane).* Industrial & Engineering Chemistry Research, 2010. 49(20): p. 9870-9876.

3. Ravi Kumar, M.N.V., *A review of chitin and chitosan applications.* Reactive and Functional Polymers, 2000. 46(1): p. 1-27.

4. Wan, Y., et al., *Biodegradable Polylactide/Chitosan Blend Membranes.* Biomacromolecules, 2006. 7(4): p. 1362-1372.

5. Tiyaboonchai, W., *Chitosan Nanoparticules: A Promising System for Drug Delivery.* Naresuan University Journal, 2003. 11(3): p. 51-66.

6. Dutta, P.K., J. Dutta, and V.S. Tripathi, *Chitin and chitosan: Chemistry, properties and applications.* Journal of Scientific & Industrial Research, 2004. 63(1): p. 20-31.

7. Wan, Y., et al., *Mechanical Properties of Porous Polylactide/Chitosan Blend Membranes.* Macromolecular Materials and Engineering, 2007. 292(5): p. 598-607.

8. Zhao, C.Z., et al., *Crystallization and thermal properties of PLLA comb polymer.* Journal of Polymer Science Part B-Polymer Physics, 2008. 46(6): p. 589-598.

9. Alves, N.M., et al., *Preparation and Characterization of New Biodegradable Films Made from Poly(L-Lactic Acid) and Chitosan Blends Using a Common Solvent.* Journal of Macromolecular Science, Part B, 2011. 50(6): p. 1121-1129.

10. Suyatma, N., et al., *Mechanical and Barrier Properties of Biodegradable Films Made from Chitosan and Poly (Lactic Acid) Blends.* Journal of Polymers and the Environment, 2004. 12(1): p. 1-6.

11. Chen, C., L. Dong, and M.K. Cheung, *Preparation and characterization of biodegradable poly(L-lactide)/chitosan blends.* European Polymer Journal, 2005. 41(5): p. 958-966.

12. Chen, J., B. Chu, and B.S. Hsiao, *Mineralization of hydroxyapatite in electrospun nanofibrous poly(L-lactic acid) scaffolds.* Journal of Biomedical Materials Research Part A, 2006. 79A(2): p. 307-317.

13. Caridade, S.G., et al., *Effect of solvent-dependent viscoelastic properties of chitosan membranes on the permeation of low molecular weight drugs.* Tissue Engineering Part A, 2008. 14(5): p. 842-842.

14. Yuan, H., X. Qiao, and J. Ren, *Synthesis and Application of Chitosan-g-PLLA Copolymers.* Journal of Macromolecular Science, Part A, 2008. 45(9): p. 754-760.

15. Arima, Y. and H. Iwata, *Effect of wettability and surface functional groups on protein adsorption and cell adhesion using well-defined mixed self-assembled monolayers.* Biomaterials, 2007. 28(20): p. 3074-3082.

16. Tamada Y., I.Y., *Polymers in Medicine II. Biomedical and Pharmaceutical Applications.* 1985, New York: N.Y. Plenum. 101-115.

17. Khor, H.L., et al., *Response of Cells on Surface-Induced Nanopatterns: Fibroblasts and Mesenchymal Progenitor Cells.* Biomacromolecules, 2007. 8(5): p. 1530-1540.

18. Lim, J. and H.-K. Park, *Fabrication of macroporous chitosan/poly(&lt;span style="font-variant:small-caps"&gt;&lt;small&gt;l&lt;/small&gt;&lt;/span&gt;-lactide) hybrid scaffolds by sodium acetate particulate-leaching method.* Journal of Porous Materials, 2012. 19(3): p. 383-387.

19. Suyatma, N.E., et al., *Mechanical and barrier properties of biodegradable films made from chitosan and poly (lactic acid) blends.* Journal of Polymers and the Environment, 2004. 12(1): p. 1-6.

20. da Silva, R.M.P., et al., *Poly(N-isopropylacrylamide) surface-grafted chitosan membranes as a new substrate for cell sheet engineering and manipulation.* Biotechnology and Bioengineering, 2008. 101(6): p. 1321-1331.

21. Kittur, F.S., et al., *Characterization of chitin, chitosan and their carboxymethyl derivatives by differential scanning calorimetry.* Carbohydrate Polymers, 2002. 49(2): p. 185-193.

22. Mucha, M. and A. Pawlak, *Thermal analysis of chitosan and its blends.* Thermochimica Acta, 2005. 427(1–2): p. 69-76.

23. Prabaharan, M., et al., *Liquid crystalline behaviour of chitosan in formic, acetic, and monochloroacetic acid solutions*, in *Advanced Materials Forum Iii, Pts 1 and 2*, P.M. Vilarinho, Editor. 2006. p. 1010-1014.

24. Sakurai, K., T. Maegawa, and T. Takahashi, *Glass transition temperature of chitosan and miscibility of chitosan/poly(N-vinyl pyrrolidone) blends.* Polymer, 2000. 41(19): p. 7051-7056.

25. Liao, Y.Z., et al., *Preparation and characterization O-lauroyl chitosan/poly (L-lactic acid) blend membranes by solution-casting approach.* Chinese Chemical Letters, 2007. 18(2): p. 213-216.

26.     Yasuniwa, M., et al., *Crystallization behavior of poly(l-lactic acid).* Polymer, 2006. 47(21): p. 7554-7563.

27.     Wu, L.B. and H.B. Hou, *Isothermal Cold Crystallization and Melting Behaviors of Poly(L-lactic acid)s Prepared by Melt Polycondensation.* Journal of Applied Polymer Science, 2010. 115(2): p. 702-708.

28.     Abe, H., et al., *Morphological and kinetic analyses of regime transition for poly (S)-lactide crystal growth.* Biomacromolecules, 2001. 2(3): p. 1007-1014.

29.     Lai, W.-C., W.-B. Liau, and T.-T. Lin, *The effect of end groups of PEG on the crystallization behaviors of binary crystalline polymer blends PEG/PLLA.* Polymer, 2004. 45(9): p. 3073-3080.

30.     Picciochi, R., et al., *Glass transition of semi-crystalline PLLA with different morphologies as studied by dynamic mechanical analysis.* Colloid & Polymer Science, 2007. 285(5): p. 575-580.

31.     Chen, C.-H., et al., *Studies of chitosan. I. Preparation and characterization of chitosan/poly(vinyl alcohol) blend films.* Journal of Applied Polymer Science, 2007. 105(3): p. 1086-1092.

32.     Silva, R.M., et al., *Preparation and characterisation in simulated body conditions of glutaraldehyde crosslinked chitosan membranes.* Journal of Materials Science-Materials in Medicine, 2004. 15(10): p. 1105-1112.

33.     Shantha, K.L. and D.R.K. Harding, *Synthesis and characterisation of chemically modified chitosan microspheres.* Carbohydrate Polymers, 2002. 48(3): p. 247-253.

34.     Pizzoli, M., G. Ceccorulli, and M. Scandola, *Molecular motions of chitosan in the solid state.* Carbohydrate Research, 1991. 222(0): p. 205-213.

35.     Lazaridou, A. and C.G. Biliaderis, *Thermophysical properties of chitosan, chitosan–starch and chitosan–pullulan films near the glass transition.* Carbohydrate Polymers, 2002. 48(2): p. 179-190.

36.     Dong, Y., et al., *Studies on glass transition temperature of chitosan with four techniques.* Journal of Applied Polymer Science, 2004. 93(4): p. 1553-1558.

# Chapter 4: Concluding Remarks

The main goal of this thesis was produce and characterizate PLLA_CHT films with different compositions of each component by a simple method that uses a common solvent (hexafluor-2-propanol). An optimization of the preparation process of the blends was successfully achieved by the elimination of the use of methanol in the precipitation of the films.

The produced films didn't present a visible phase separation. FTIR and OM analysis evidenced that the blends also presented a good miscibility at the microscopic level, for all the studied compositions. Swelling tests evidenced that the films with the highest amount of CHT presented a higher swelling ratio. Regarding contact angle measurements, the wetability of the blends increased as the CHT content increased. SEM showed that all the films presented a rough surface, somewhat different depending on the composition, being PLLA50_CHT50 rougher than the other blends.

DSC showed that the presence of CHT in the blends affected significantly the cold crystallization and the isothermal crystallization behaviour of the PLLA fraction, almost preventing crystallization when the CHT fraction is equal or above 50%.

DMA scans temperature results evidenced that E' increased as the PLLA content in the blends increased and that the $T_g$ of PLLA decreased when the CHT fraction increased, probably to a plasticizer effect. The DMA unconventional tests allowed to analyse the glass transition process of the CHT fraction of the blends. A shift of the $T_g$ of the CHT fraction towards lower water content was found, from 26% to 20% when the PLLA content increased from 25% to 50.% It was also possible to conclude that the storage modulus of the blends decreased with the increase of water content.

This work allowed the learning process of several characterization techniques, in particular the DMA technique which by itself is very difficult to work with.

As future works, PLLA/CHT films should be produced and their properties should be evaluated in terms of biological performance.
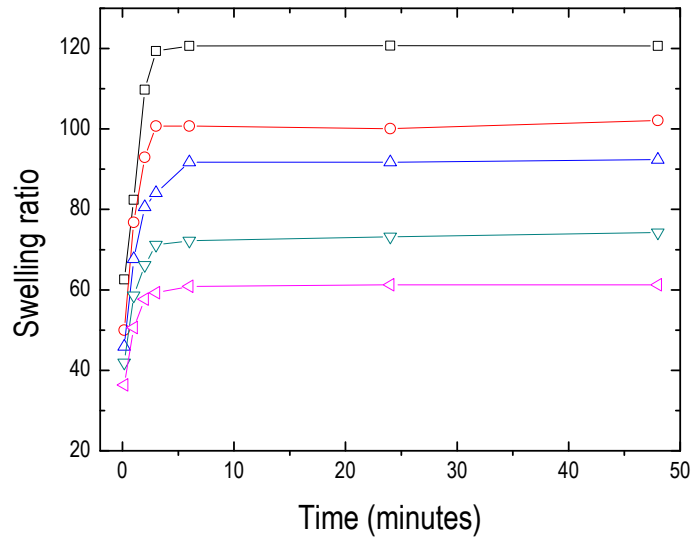
# Annex 1



Figure 1. Dependence of the time of the swelling ratio. [CHT ( □ ), PLLA25_CHT75 ( ○ ), PLLA50_CHT50 ( △ ),
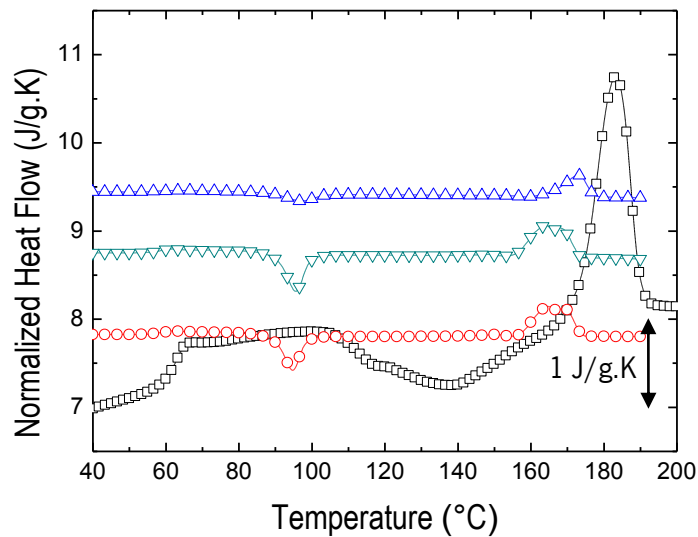PLLA75_CHT25 ( ▽ ), PLLA ( ◁ )].



Figure 2. DSC thermogram of PLLA/CHT films produced with methanol in their precipitation [ PLLA ( –□– ),
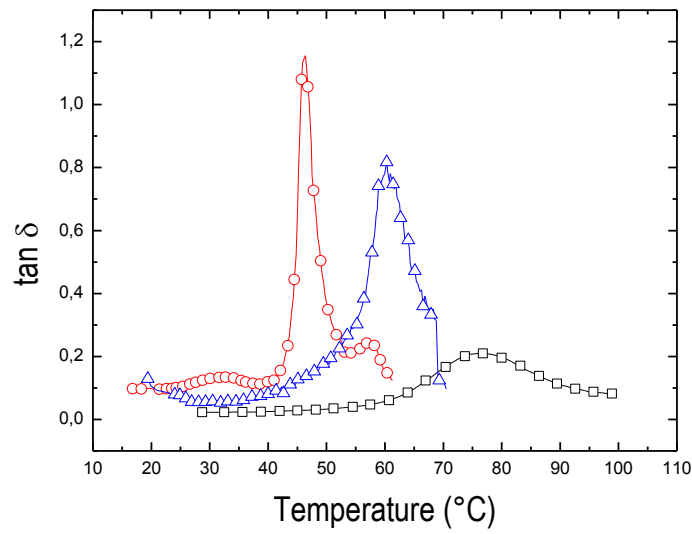PLLA75_CHT25( –○– ), PLLA50_CHT50 ( –△– ), PLLA25_CHT75 ( –▽– )]

Figure 3. Damping factor (tan δ) as a function of temperature of PLLA/CHT films. [PLLA ( —☐— ), PLLA75_CHT25 (—O—), PLLA50_CHT50 (—△—)].
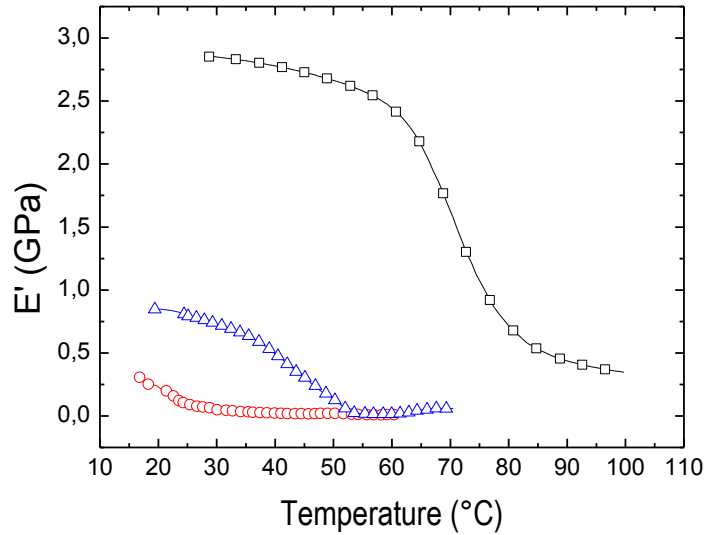


Figure 4. Storage modulus(*E'*) as a function of temperature of PLLA/CHT films. [PLLA ( —☐— ), PLLA75_CHT25 (—△—), PLLA50_CHT50 (—O—)].
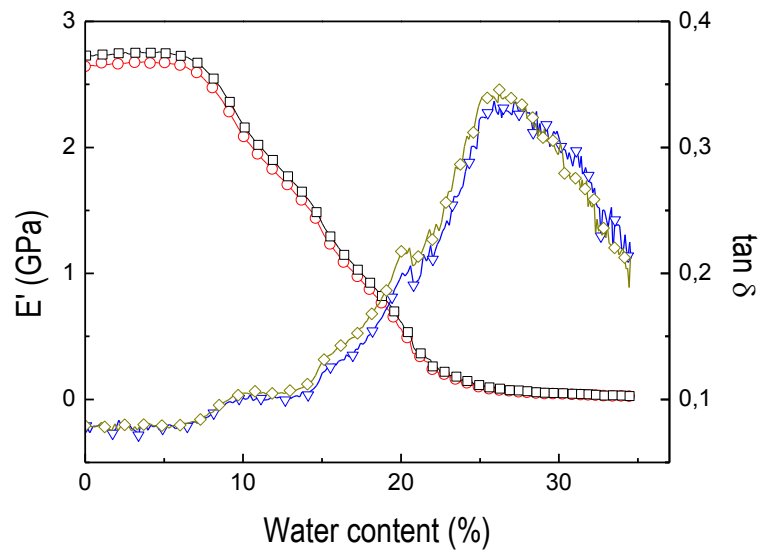
Figure 5. Apparent storage modulus (*E'*) and loss factor (tan δ) at room temperature measured with samples immersed in water/ethanol mixtures as a function of water content of PLLA25_CHT75 film.[ E'_1Hz (—▫—), E'_0.5Hz (—O—), tan δ_1Hz ( —▽— ), tan δ_0.5Hz(—◇—)].